

https://doi.org/10.3799/dqkx.2021.140



# 镁同位素地球化学研究新进展及其在碳酸岩研究中的应用

陈洁<sup>1</sup>, 龚迎莉<sup>2</sup>, 陈露<sup>1\*</sup>, 向蜜<sup>1</sup>, 田世洪<sup>1,3</sup>

1. 东华理工大学核资源与环境国家重点实验室, 江西南昌 330013

2. 清华大学能源与动力工程系, 北京 100084

3. 自然资源部成矿作用与资源评价重点实验室, 中国地质科学院矿产资源研究所, 北京 100037

**摘要:** 镁(Mg)同位素有 3 个, <sup>24</sup>Mg、<sup>25</sup>Mg 和 <sup>26</sup>Mg, 其中 <sup>24</sup>Mg 和 <sup>26</sup>Mg 的相对质量差较大, 高达 8.33%, 这种大的相对质量差使地壳活动或其他地质过程中 Mg 同位素因化学物理条件的变化而发生明显的同位素质量分馏。目前, 自然界可观测到的  $\delta^{26}\text{Mg}$  变化范围为  $-5.60\text{‰}$ ~ $0.92\text{‰}$ , 约 6.5‰。镁在低温地球化学过程中分馏显著, 而在高温环境下分馏不明显, 因而 Mg 同位素是地质过程的潜在地球化学指标和示踪剂, 在低温风化作用、高温部分熔融与岩浆结晶分异、变质作用、板片俯冲及壳幔物质循环、热液蚀变和矿床成因等方面取得重要进展。为此, 简要介绍了镁同位素分析方法, 系统总结了 Mg 同位素在地球各储库中的组成与分布特征以及地质作用过程中的镁同位素分馏机理; 其次重点介绍了镁同位素近年来在碳酸岩研究中的应用; 最后对有关问题进行了探讨, 包括幔源岩石低  $\delta^{26}\text{Mg}$  成因解释(与俯冲再循环的碳酸盐岩、洋壳物质有关或与矿物分离结晶有关)和 Li-Mg-Ca 同位素联合示踪岩浆碳酸岩岩石成因。并对碰撞反应池多接收器电感耦合等离子体质谱仪(Nu Sapphire MC-ICP-MS)分析优势和 Li-Mg-Ca 等金属同位素联合示踪在稀土元素富集机制的应用进行了展望。

**关键词:** 镁同位素; 分析方法; 同位素分馏; 联合示踪; 碳酸岩; 地球化学。

中图分类号: P597.2

文章编号: 1000-2383(2021)12-4366-24

收稿日期: 2021-06-11

## New Advances in Magnesium Isotope Geochemistry and Its Application to Carbonatite Rocks

Chen Jie<sup>1</sup>, Gong Yingli<sup>2</sup>, Chen Lu<sup>1\*</sup>, Xiang Mi<sup>1</sup>, Tian Shihong<sup>1,3</sup>

1. State Key Laboratory of Nuclear Resources and Environment, East China University of Technology, Nanchang 330013, China

2. Department of Energy and Power Engineering, Tsinghua University, Beijing 100084, China

3. MNR Key Laboratory of Metallogeny and Mineral Assessment, Institute of Mineral Resources, Chinese Academy of Geological Sciences, Beijing 100037, China

**Abstract:** There are three magnesium (Mg) isotopes, <sup>24</sup>Mg, <sup>25</sup>Mg and <sup>26</sup>Mg, among which the relative mass difference of <sup>26</sup>Mg and <sup>24</sup>Mg is large, up to 8.33%. Such a large relative mass difference can cause significant mass dependent fractionation of Mg isotopes due to the changes of chemical and physical conditions during crustal activities or other geological processes. Variations of  $\delta^{26}\text{Mg}$  in nature are mainly from  $-5.60\text{‰}$  to  $0.92\text{‰}$ , spanning a limited range of 6.5‰. Mg isotope is a potential geochemical index and tracer for geological processes because Mg fractionates significantly in low-temperature geochemical processes, but not in high-

**基金项目:** 国家自然科学基金(No.41773014); 江西省“双千计划”创新领军人才长期项目、东华理工大学博士启动基金(No.DHBK2020012); 高层次人才引进配套经费(No.1410000874)。

**作者简介:** 陈洁(1998-), 女, 硕士, 主要从事同位素地球化学和矿床学研究工作。ORCID:0000-0001-9987-9315。E-mail: chenjieswx@163.com

\* **通讯作者:** 陈露, E-mail: luchennwu@163.com

**引用格式:** 陈洁, 龚迎莉, 陈露, 等, 2021. 镁同位素地球化学研究新进展及其在碳酸岩研究中的应用. 地球科学, 46(12):4366-4389.

temperature environments. Mg isotopes have made important progress in the fields of low-temperature weathering, high-temperature partial melting and magmatic crystallization differentiation, metamorphism, plate subduction, crust-mantle material recycling, hydrothermal alteration and genesis of deposits. In this paper, the analysis methods of Mg isotopes are briefly introduced firstly. Secondly, the composition and distribution characteristics of Mg isotopes in various reservoirs of the earth and the fractionation mechanism of Mg isotopes in geological processes are systematically summarized. And then, the application of magnesium isotopes in the study of carbonatites in recent years is emphatically introduced. Finally, it discusses the origin of low  $\delta^{26}\text{Mg}$  in mantle-derived rocks (related to carbonate rocks of subduction and recycling, oceanic crust materials or mineral separation crystallization) and trace the petrogenesis of magmatic carbonatites by the combination of Li, Mg and Ca isotopes. At the end of this paper, the advantages of the dual-path collision cell-capable multiple-collector inductively coupled plasma mass spectrometer (Nu Sapphire MC-ICP-MS) and the application of Li-Mg-Ca and other metal isotopes in the enrichment mechanisms of rare earth elements are prospected.

**Key words:** magnesium isotope; analytical method; isotope fractionation; combined tracer; carbonatites; geochemistry.

## 0 引言

镁是一种主量元素,标准原子量为 $[24.304, 24.307]$ (CIAAW, 2019),克拉克值为 $2.4 \times 10^4 \text{ mg/kg}$ (陆壳) $\sim 4.3 \times 10^4 \text{ mg/kg}$ (洋壳)(范百龄等, 2013). 地球上的镁以 MgO 的形式大量赋存于地幔中(图 1a; Teng, 2017). Mg 是极易迁移的水溶性元素,具有活跃的地球化学性质. 高温下 Mg 作为难熔元素富集于残留相,而结晶分异过程中 Mg 优先进入矿物相(Teng, 2017; 苏本勋等, 2018). 在火成岩中, Mg 主要以硅酸盐矿物形式(橄榄石、辉石、角闪石、石榴石、云母、尖晶石等)存在于玄武岩、橄榄岩或以碳酸盐矿物形式(白云石、方解石等)存在于碳酸岩中(Teng, 2017). 天然镁同位素有 3 个,分别为  $^{24}\text{Mg}$ 、 $^{25}\text{Mg}$  和  $^{26}\text{Mg}$ , 均为稳定同位素,丰度分别为 78.99%、10.00% 和 11.01% (图 1b; Teng, 2017).  $^{26}\text{Mg}$  和  $^{24}\text{Mg}$  相对质量差为 8.33%, 这种大的相对质量差会使地壳活动或其他地质过程中的 Mg 同位素因化学物理条件的变化而发生明显的同位素质量分馏(Guo *et al.*, 2019).

Mg 同位素最早应用于天体学科中,由于分析技术的局限性,研究大多集中在与同位素非质量分馏相关的镁同位素异常上( $^{26}\text{Al}$ - $^{26}\text{Mg}$  体系)(Gray and Compston, 1974; Lee and Papanastassiou, 1974; Heymann and Dziczkaniec, 1976). 近年来,随着分析方法的改进和现代质谱仪器的发展,多接收电感耦合等离子体质谱仪(MC-ICP-MS)可精确测量地质样品中的镁同位素组成,而激光与 MC-ICP-MS 的联用也使矿物样品的原位镁同位素分析成为可能(Teng *et al.*, 2007; 李世珍等, 2008; Oeser *et al.*,

2015; 戴梦宁等, 2016). 新分析技术的出现加快了镁同位素分馏的研究进程,拓展了镁同位素在地质领域的应用.

研究表明,在高温部分熔融(Teng *et al.*, 2010a; 李曙光, 2015; 肖益林等, 2015; An *et al.*, 2017)、玄武岩浆结晶分异(Yang *et al.*, 2009; Huang *et al.*, 2011; Liu *et al.*, 2011; Xiao *et al.*, 2013; Hu *et al.*, 2016; Wang *et al.*, 2016a)、花岗岩浆结晶分异(Li *et al.*, 2010; Liu *et al.*, 2010; Teng *et al.*, 2013; Ke *et al.*, 2016)、变质作用(Li *et al.*, 2011; Teng *et al.*, 2013; Tian *et al.*, 2020a)等高温岩浆作用过程中镁同位素不发生有意义的分馏,但在硅酸盐风化(Li *et al.*, 2010; Wimpenny *et al.*, 2014a, 2014b; Gao *et al.*, 2018; Oskierski *et al.*, 2019; Pogge von Strandmann *et al.*, 2019; Hindshaw *et al.*, 2020; Li *et al.*, 2021a)和碳酸盐溶解沉淀(Geske *et al.*, 2015; 董爱国和朱祥坤, 2016; Teng, 2017; Bialik *et al.*, 2018; Hindshaw *et al.*, 2019; Zhao *et al.*, 2019; Li *et al.*, 2020; Harrison *et al.*, 2021; Jin *et al.*, 2021; Shalev *et al.*, 2021)这两大低温地球化学过程中分馏显著.

镁同位素地球化学是一个年轻的研究领域,但在如下方面取得了重要进展:表生环境低温风化作用过程(Teng *et al.*, 2010b; 范百龄等, 2013; Lee *et al.*, 2014; Dessert *et al.*, 2015; 董爱国和朱祥坤, 2016; 董爱国和韩贵琳, 2017; Teng, 2017; Brewer *et al.*, 2018; Gao *et al.*, 2018; Fries *et al.*, 2019; Hindshaw *et al.*, 2019, 2020; Nitzsche *et al.*, 2019; Oskierski *et al.*, 2019; Tian *et al.*, 2019; Chen *et al.*, 2020a; Ryu *et al.*, 2021)、高温部分熔融与岩浆结晶分异过程(Hu *et al.*, 2016; Li *et al.*, 2016; Wang *et al.*,

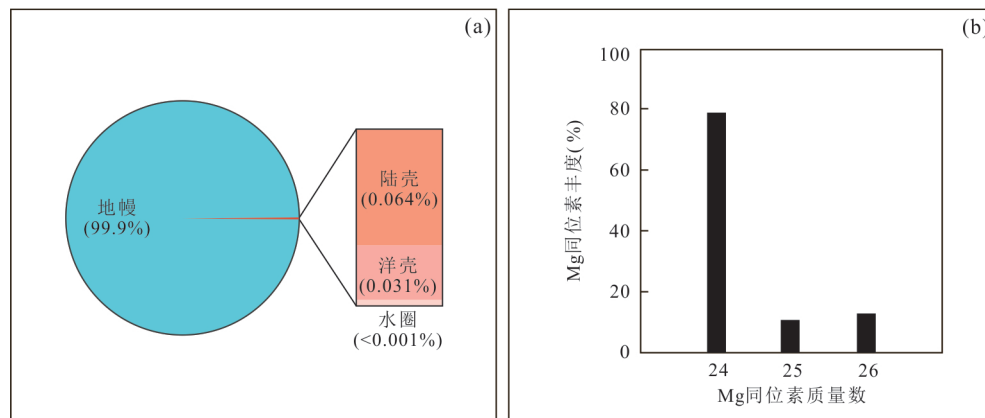


图1 地幔、陆壳、洋壳和水圈中Mg的质量分数(a);镁同位素的质量数和天然丰度(b)(据 Teng, 2017)

Fig.1 Mass fraction of Mg in the mantle, continental crust, oceanic crust and hydrosphere (a), Mass number and natural abundance of Mg isotopes (b) (modified after Teng, 2017)

2016a; An *et al.*, 2017; Cheng *et al.*, 2017; Song *et al.*, 2017; Su *et al.*, 2017a; Zhong *et al.*, 2017; Jung *et al.*, 2019; Su *et al.*, 2019a; Chen *et al.*, 2020b; Pang *et al.*, 2020)、变质作用过程(Li *et al.*, 2011; Teng *et al.*, 2013; Li *et al.*, 2014; Wang *et al.*, 2015a; Hu *et al.*, 2017a; Tian *et al.*, 2020a)、板片俯冲及壳幔物质循环(Yang *et al.*, 2012; Ling *et al.*, 2013; Wang *et al.*, 2014a, 2014b; Huang *et al.*, 2015a; 肖益林等, 2015; Huang and Xiao, 2016; Li *et al.*, 2016; Song *et al.*, 2016; Teng *et al.*, 2016; Cheng *et al.*, 2017; Song *et al.*, 2017; Su *et al.*, 2017b; Sun *et al.*, 2017; Wang *et al.*, 2017a, 2017b; Hoang *et al.*, 2018; Wang *et al.*, 2018; Xie *et al.*, 2018; Jung *et al.*, 2019; Kim *et al.*, 2019; 沈骥等, 2019; Tian *et al.*, 2019; Chen *et al.*, 2020c; Dai *et al.*, 2020; Tian *et al.*, 2020b; Li *et al.*, 2021b)、热液蚀变(Huang *et al.*, 2015b; Hu *et al.*, 2019; 李伟强等, 2020)、矿床成因(Ling *et al.*, 2013; Song *et al.*, 2016; 苏本勋等, 2018; Tang *et al.*, 2018; 李伟强等, 2020)等。尽管镁同位素在上述领域取得诸多研究成果, 但 Teng (2017)认为镁同位素地球化学仍处于起步阶段, 未来的研究将惠及更多领域。

本文首先简要介绍了镁同位素分析方法, 其次总结了各主要储库的镁同位素组成和地质作用过程中的镁同位素分馏行为及机制, 最后重点介绍了镁同位素在碳酸岩中的应用、幔源岩石低 $\delta^{26}\text{Mg}$ 的成因解释和Li-Mg-Ca同位素联合示踪岩浆碳酸岩岩石成因, 以供感兴趣的专家、学者和研究生参考, 希望对今后镁同位素研究有一定的借鉴作用。

## 1 Mg同位素分析方法

Mg同位素组成用样品和国际标样的Mg同位素比值的千分偏差表示:  $\delta^{26}\text{Mg}(\text{‰}) = [({}^{26}\text{Mg}/{}^{24}\text{Mg})_{\text{样品}}/({}^{26}\text{Mg}/{}^{24}\text{Mg})_{\text{标样}} - 1] \times 1000$ , Mg同位素的测定常以DSM3作为标准物质(Teng, 2017; Teng *et al.*, 2017)。

### 1.1 标准物质

国际上Mg同位素的标准物质是纯镁金属的硝酸溶液: SRM980、DSM3、Cambridge-1。DSM3(Dead Sea Magnesium Ltd., Israel)是用10 g纯金属Mg以0.3 N  $\text{HNO}_3$ 为介质制备的1%硝酸镁溶液。DSM3和Cambridge-1的Mg同位素组成均一, 但相比之下, DSM3的Mg同位素组成与碳质球粒陨石基本一致, 具有宇宙和地球化学意义(Galy *et al.*, 2003; 张宏福等, 2007; Bolou-Bi *et al.*, 2009)。SRM980的Mg同位素组成很不均一, 不适合作为Mg同位素高精度测量的标准物质, 国际上已将其弃用(Galy *et al.*, 2003; Teng, 2017; Teng *et al.*, 2017)。因此, 国际上广泛使用DSM3作为Mg同位素组成测定的标准物质。国内实验室常用的内部标准物质有CAGS1-Mg和CAGS2-Mg(何学贤等, 2008)以及GSB(Gao *et al.*, 2019)。Vega *et al.*(2020)证明了可用新标样ERM-AE143(Federal Institute for Materials Research and Testing BAM, Berlin, Germany)作为镁的新同位素标准物质用来替代紧缺的DSM3标样。

### 1.2 Mg的化学分离提纯

对于岩石样品, 不同研究者使用的消解样品方法大同小异(Teng *et al.*, 2007; 何学贤等, 2008; 李

表 1 不同标样相对于 DSM3 的值  
Table 1 Values of different standard samples relative to DSM3

标样	$\delta^{26}\text{Mg}$	$\delta^{25}\text{Mg}$	参考文献
SRM980	$-3.980\% \pm 0.050\%$	$-2.040\% \pm 0.050\%$	Bolou-Bi <i>et al.</i> , 2009
Cambridge-1	$-2.623\% \pm 0.030\%$	$-1.358\% \pm 0.030\%$	Teng <i>et al.</i> , 2015
CAGS1-Mg	$0.399\% \pm 0.100\%$	$0.200\% \pm 0.050\%$	何学贤等, 2008
CAGS2-Mg	$0.270\% \pm 0.100\%$	$0.150\% \pm 0.050\%$	何学贤等, 2008
GSB	$-2.032\% \pm 0.038\%$	$-1.044\% \pm 0.024\%$	Gao <i>et al.</i> , 2019
ERM-AE143	$-3.295\% \pm 0.040\%$	$-1.666\% \pm 0.043\%$	Vega <i>et al.</i> , 2020

世珍等, 2008; Huang *et al.*, 2009; Teng *et al.*, 2010a, 2010b, 2015; Gao *et al.*, 2019; Wang *et al.*, 2020). Mg 同位素在淋洗过程中易发生较大的同位素分馏, 在质谱分析之前, 需要彻底分离基体元素, 尽可能使分离纯化流程的回收率接近 100%, 以减小基体效应的影响 (Chang *et al.*, 2003; Oi and Kakihana, 1987; Huang *et al.*, 2009). Mg 的分离所采用的离子交换树脂包括 AG50W-X12 阳离子交换树脂 (李伟强等, 2020; Zhong *et al.*, 2021)、AG50W-X8 阳离子交换树脂 (Teng *et al.*, 2007, 2010a, 2010b, 2015; Teng, 2017; Gao *et al.*, 2019; Pang *et al.*, 2020; Tian *et al.*, 2020a, 2020b; Wang *et al.*, 2020) 和 AGMP-1 阴离子交换树脂 (孙剑等, 2012). 分离过程中使用不同浓度的稀 HCl 或 HNO<sub>3</sub> 依次淋洗分离 Mg 和基体元素 (Ling *et al.*, 2013; Hoang *et al.*, 2018). 对于特殊的高基体样品, 一般还会使用化学沉淀法将 Mg 与基体元素分离 (主要去除 Fe、Al 和 K 等; 李世珍等, 2008; Bao *et al.*, 2020). 由于天然样品基体差异大, 同一流程纯化的样品可能有不同元素的残留, 各实验室都会进行基体效应实验以评估样品中残留基体元素对测试的影响. 例如, 何学贤等 (2008) 的实验结果表明控制 [Na、Ca、Al、Fe 或 Cr]/[Mg] 的浓度比小于 0.05 时, 基体效应不明显 (Nu Plasma HR, 干法); 李瑞瑛等 (2016) 的实验结果证明溶液中 Cr/Mg  $\leq 0.5$  时, 对测试结果没有影响 (Neptune Plus, 湿法); Gao *et al.* (2019) 的实验结果表明溶液中 Na/Mg  $\geq 0.4$ , Ca/Mg  $\geq 1.5$ , Ti/Mg  $> 0.1$  会导致  $\delta^{26}\text{Mg}$  值不准确 (Neptune Plus, 湿法).

### 1.3 Mg 同位素测定

早期 Mg 同位素组成测量技术为热电离质谱 (TIMS) 和二次离子质谱 (SIMS), 仪器测量精度最高只能达到 1%, 无法识别地质样品 Mg 同位素组成的变化, 极大制约了 Mg 同位素的应用研究 (范百龄等, 2013; Teng and Yang, 2014; Teng, 2017; Bao

*et al.*, 2020). MC-ICP-MS 的出现使得高精度镁同位素测量成为可能. 目前 Mg 同位素组成主要通过溶液法 MC-ICP-MS 进行测定. MC-ICP-MS 技术的发展和完善, 大大提高了 Mg 同位素的分析精度 ( $\delta^{25}\text{Mg}$  和  $\delta^{26}\text{Mg}$  分别达 0.06‰ 和 0.12‰), 而且灵敏度也有显著的提高 (样品量可以少到  $0.5 \times 10^{-6}$  g) (范百龄等, 2013). Galy *et al.* (2001) 通过“标准—样品交叉法” (SSB) 进行了 Mg 同位素的首次高精度分析. 近年来, 随着分析方法的改进和现代质谱仪器的发展, 越来越多的学者运用 MC-ICP-MS 进行 Mg 同位素高精度分析并开展有关的地球化学研究 (An *et al.*, 2014; Teng and Yang, 2014; Tang *et al.*, 2018; Wu *et al.*, 2018; Xie *et al.*, 2018; 陈伊翔, 2019; Jung *et al.*, 2019; Oskierski *et al.*, 2019; 沈骥等, 2019; Su *et al.*, 2019a; Tian *et al.*, 2019; Bao *et al.*, 2020). MC-ICP-MS 测定 Mg 同位素需要注意以下问题: (1) 浓度与酸度影响: 样品溶液与标准样品溶液中 Mg 的浓度差异需控制在 10% 以内, 介质酸浓度应保持一致 (An *et al.*, 2014; Teng and Yang, 2014; 戴梦宁等, 2016; 李瑞瑛等, 2016; Gao *et al.*, 2019); (2) 储存影响: 长期在聚丙烯或高密度聚乙烯瓶中储存高浓度镁溶液标准物质 (约  $500 \times 10^{-6}$ ), 不会导致同位素组成变化; 而特氟龙 (PTFE) 瓶会使低浓度镁标准溶液 ( $0.2 \times 10^{-6}$ ) 的  $\delta^{26}\text{Mg}$  产生约 0.2‰ 的负偏差, 可能是由于容器吸附了重 Mg 同位素或从容器中浸出了有机质 (Huang *et al.*, 2009); (3) 温度影响: 温差过大会使仪器质量偏差产生非线性变化从而影响同位素分析的准确性, 因此需保持长期稳定的室温 (4 °C 的温差可导致约 0.9‰ 的误差; Gao *et al.*, 2019). 随着 Mg 同位素地质应用的发展, 矿物微区同位素组成越来越受到重视, 不少研究者尝试开发激光剥蚀与 MC-ICP-MS 联用原位 Mg 同位素分析方法 (Xie *et al.*, 2011; Sio *et al.*, 2013; Oeser *et al.*, 2014; 戴梦宁等, 2016; Chauss-

idon *et al.*, 2017). 相对于溶液进样的 MC-ICP-MS, 虽然原位分析的精度仅有 1‰~2‰ (戴梦宁等, 2016), 但其在矿物微区 (环带) Mg 同位素组成研究方面已取得显著成果 (戴梦宁等, 2016; Chaussidon *et al.*, 2017; Teng, 2017).

## 2 地球主要储库 Mg 同位素组成

根据最近几年发表的主要研究成果, 比较全面总结了主要储库的 Mg 同位素组成 (图 2).

Guo *et al.* (2019) 统计得出地幔橄榄岩  $\delta^{26}\text{Mg} = -0.51\text{‰} \sim -0.03\text{‰}$ , 平均值为  $-0.21\text{‰}$ ; 地幔玄武岩  $\delta^{26}\text{Mg} = -0.57\text{‰} \sim -0.06\text{‰}$ , 平均值为  $-0.27\text{‰}$ . 原始地幔  $\delta^{26}\text{Mg} = -0.25\text{‰} \pm 0.07\text{‰}$  (Teng *et al.*, 2010a). 球粒陨石具有相似的镁同位素组成, 表明太阳系具有均匀的 Mg 同位素组成 (Chakrabarti and Jacob-

sen, 2010). Guo *et al.* (2019) 统计得出球粒陨石  $\delta^{26}\text{Mg} = -0.38\text{‰} \sim -0.15\text{‰}$ , 平均值为  $-0.28\text{‰}$ , 与地幔的基本一致. 洋底玄武岩熔岩  $\delta^{26}\text{Mg} = -0.32\text{‰} \sim -0.15\text{‰}$  (Zhong *et al.*, 2021). 迄今为止, 报道的碳酸岩镁同位素组成大多偏离了原始地幔值, 其中钙质碳酸岩  $\delta^{26}\text{Mg} = -2.28\text{‰} \sim -0.23\text{‰}$ , 具有较大的变化范围 (Ling *et al.*, 2013); 镁质碳酸岩  $\delta^{26}\text{Mg} = -1.09\text{‰} \sim -0.85\text{‰}$ , 具有远低于地幔的轻镁同位素特征 (Cheng *et al.*, 2017); 钠质碳酸岩  $\delta^{26}\text{Mg} = 0.13\text{‰} \sim 0.37\text{‰}$ , 具有正  $\delta^{26}\text{Mg}$  特征 (Li *et al.*, 2016).

地球最外层 (陆壳、洋壳和水圈) 中镁含量在整个地球中占比不到 0.1% (图 1a), 但镁同位素分馏大于 6‰ (Wimpenny *et al.*, 2014a, 2014b; Wang *et al.*, 2015b; Teng, 2017; Guo *et al.*, 2019). 整体陆

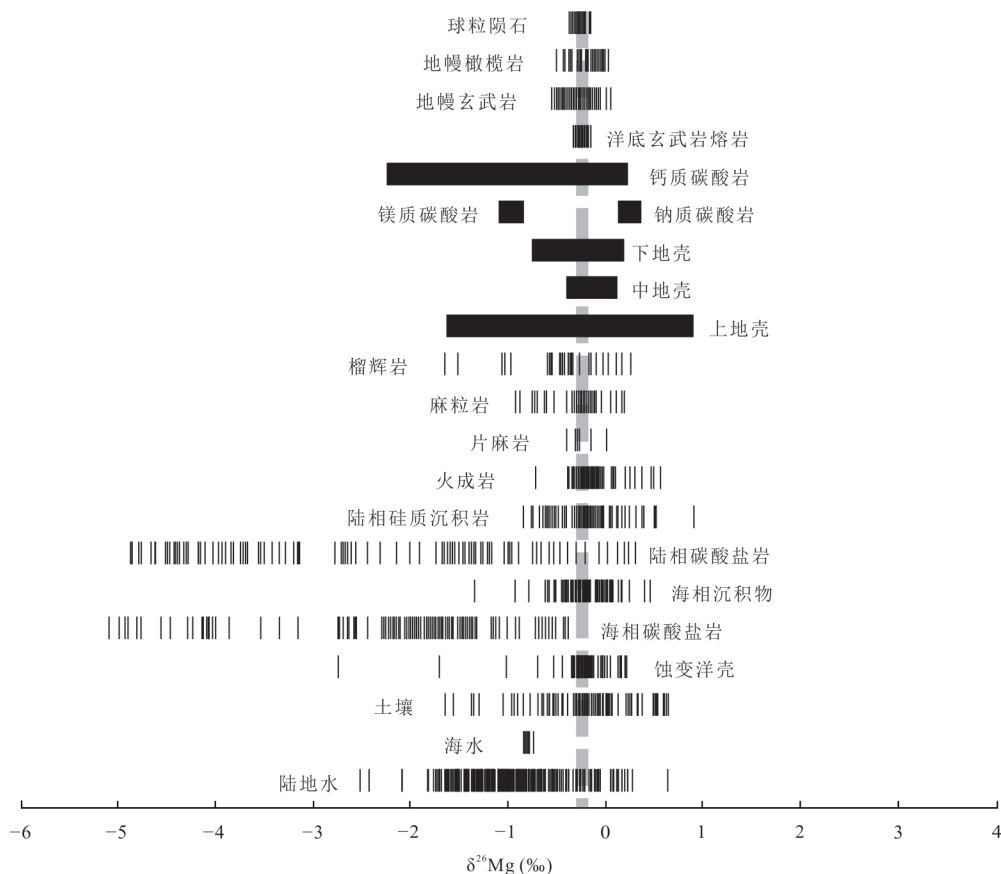


图 2 地球不同储库的镁同位素组成 (灰色虚线代表原始地幔的平均  $\delta^{26}\text{Mg} = -0.25\text{‰} \pm 0.07\text{‰}$ )

Fig. 2 Mg isotopic compositions of different reservoirs in the Earth system (the gray dashed line represents the average  $\delta^{26}\text{Mg}$  of  $-0.25\text{‰} \pm 0.07\text{‰}$  for the pristine mantle)

据 Tipper *et al.* (2006); Teng *et al.* (2010a); Huang *et al.* (2013); Ling *et al.* (2013); Teng *et al.* (2013); Li *et al.* (2016); Yang *et al.* (2016); Cheng *et al.* (2017); 董爱国和韩贵琳 (2017); Hu *et al.* (2017b); Huang *et al.* (2018); Guo *et al.* (2019); 黄建等 (2019); He *et al.* (2020); Ryu *et al.* (2021); Zhong *et al.* (2021) 修改

壳平均  $\delta^{26}\text{Mg}$  为  $-0.24\%$ , 类似于地幔 (Yang *et al.*, 2009; Teng *et al.*, 2010a; Pogge von Strandmann *et al.*, 2011; Sedaghatpour and Teng, 2016; Teng, 2017). 大陆下地壳  $\delta^{26}\text{Mg} = -0.76\% \sim 0.19\%$  (Teng *et al.*, 2013; Yang *et al.*, 2016); 大陆中地壳  $\delta^{26}\text{Mg} = -0.40\% \sim 0.12\%$  (Yang *et al.*, 2016); 大陆上地壳  $\delta^{26}\text{Mg} = -1.64\% \sim 0.92\%$  (Huang *et al.*, 2013). Guo *et al.* (2019) 统计得出榴辉岩  $\delta^{26}\text{Mg} = -1.66\% \sim 0.26\%$ , 平均值为  $-0.31\%$ ; 麻粒岩  $\delta^{26}\text{Mg} = -0.93\% \sim 0.19\%$ , 平均值为  $-0.27\%$ ; 片麻岩  $\delta^{26}\text{Mg} = -0.40\% \sim -0.05\%$ , 平均值为  $-0.27\%$ ; 火成岩  $\delta^{26}\text{Mg} = -0.75\% \sim 0.55\%$ , 平均值为  $-0.23\%$ . 沉积物中碳酸盐岩的镁同位素组成较轻、处于轻镁端元 (低至  $-5.6\%$ ; Teng, 2017), 而硅酸盐的镁同位素组成较重, 位于重镁端元新鲜花岗岩  $\delta^{26}\text{Mg} = 0.35\% \sim 0.69\%$  (Lee *et al.*, 2018); 风化硅酸盐  $\delta^{26}\text{Mg}$  可高达  $1.80\%$  (Liu *et al.*, 2014). 陆相硅质沉积岩  $\delta^{26}\text{Mg} = -0.86\% \sim 0.90\%$ , 平均值为  $-0.15\%$ ; 而陆相碳酸盐岩  $\delta^{26}\text{Mg} = -4.87\% \sim 0.28\%$ , 平均值为  $-2.45\%$  (Guo *et al.*, 2019). 海相沉积物 (主要成分为陆源硅酸盐碎屑)  $\delta^{26}\text{Mg} = -1.34\% \sim 0.46\%$ , 与陆相硅质沉积岩的相似, 这可能与沉积物岩性有关, 其中富碳酸盐岩沉积物富集轻 Mg 同位素, 而富粘土 (硅酸盐) 沉积物普遍富集重 Mg 同位素 (Hu *et al.*, 2017b). 海相碳酸盐岩具有明显低的  $\delta^{26}\text{Mg}$  值,  $\delta^{26}\text{Mg} = -5.10\% \sim -0.39\%$  (Guo *et al.*, 2019; He *et al.*, 2020). 蚀变洋壳  $\delta^{26}\text{Mg} = -2.76\% \sim 0.21\%$ , 变化范围较大 (Huang *et al.*, 2018; 黄建等, 2019). 土壤  $\delta^{26}\text{Mg} = -1.64\% \sim 0.65\%$  (Guo *et al.*, 2019; Ryu *et al.*, 2021). 海水的镁同位素组成均一, Guo *et al.* (2019) 统计得出海水  $\delta^{26}\text{Mg} = -0.87\% \sim -0.77\%$ , 平均值为  $-0.84\%$ . 陆地水 (地表水和地下水, 以河水为主)  $\delta^{26}\text{Mg} = -2.52\% \sim 0.64\%$ , 平均值约为  $-1.09\%$  (Tipper *et al.*, 2006; 董爱国和韩贵琳, 2017).

### 3 Mg 同位素分馏

#### 3.1 Mg 同位素平衡分馏

稳定同位素平衡分馏的根本原因是不同的分子具有不同的零点振动能, 随着温度升高, 不同分子之间的零点振动能之差减小 (Urey, 1947). 若温度接近无限高, 任何两相之间的零点振动能量之差将趋于无限小, 同位素分馏也将变得无限小. 因此,

地球表面低温条件下镁同位素平衡分馏显著 (Teng *et al.*, 2010b), 而高温岩浆过程中镁同位素平衡分馏通常很小 (Li *et al.*, 2011; An *et al.*, 2017; Teng, 2017; Luo *et al.*, 2020). 此外, 除温度外, 压力对矿物间镁同位素平衡分馏也有显著影响 (矿物间镁同位素平衡分馏与压力呈负相关; Chen *et al.*, 2020b).

研究表明, 同位素平衡分馏受矿物中 Mg 的配位数控制, 重同位素倾向于进入低配位数的矿物 (Teng, 2017; Guo *et al.*, 2019; Antonelli and Simon, 2020). 配位数越高, 键长越长, 键能越弱, 而重同位素优先聚集在短化学键中. 因此, 具有低 Mg 配位数的矿物往往富含重 Mg 同位素组成 (Liu *et al.*, 2010). 橄榄石 (Ol)、斜方辉石 (Opx)、单斜辉石 (Cpx)、角闪石 (Hbl)、黑云母 (Bt) 中 Mg 的配位数都是 6, 而在尖晶石 (Spl) 中是 4, 石榴石 (Grt) 中是 8 (Teng, 2017). 因此, 共存的 Ol、Opx、Cpx、Hbl 和 Bt 间的 Mg 同位素分馏有限, Spl 的 Mg 同位素组成较重, 而 Grt 的 Mg 同位素组成较轻. 经实验校准, 在共存造岩矿物的平衡镁同位素分馏中,  $^{26}\text{Mg}$  富集的顺序为:  $\text{Spl} > \text{Bt} > \text{Hbl} \approx \text{Cpx} > \text{Opx} > \text{Ol} \geq \text{Grt}$ , 与理论推测和定性计算相符 (Schauble, 2011; Macris *et al.*, 2013; Teng, 2017). 地幔捕虏体中共存的 Ol、Opx、Cpx (Handler *et al.*, 2009; Xiao *et al.*, 2013; Lai *et al.*, 2015; Hu *et al.*, 2016; Wang *et al.*, 2016a) 和花岗岩类中共存的 Hbl 和 Bt (Liu *et al.*, 2011) 的矿物间平衡分馏小于  $0.2\%$  (Teng, 2017; Bai *et al.*, 2021). Ol 和 Opx 之间的镁同位素分馏小于  $0.1\%$ , 可忽略不计 (Bai *et al.*, 2021), Ol 和 Cpx 的分离结晶会产生小于  $\pm 0.07\%$  平衡镁同位素分馏 (Teng *et al.*, 2007, 2010a; Li *et al.*, 2010; Liu *et al.*, 2010; Wang *et al.*, 2021). 通过对火成岩和变质岩中的这些矿物的  $\delta^{26}\text{Mg}$  测量, 确实发现了包括尖晶石和石榴石在内的大量平衡矿物间分馏 (Xiao *et al.*, 2013; Wang *et al.*, 2015a, 2015b; Hu *et al.*, 2016; An *et al.*, 2017).

碳酸盐和硅酸盐矿物的共生体系中存在矿物间的平衡镁同位素分馏, 重镁同位素相对于碳酸盐熔体优先分配到硅酸盐熔体中 (Schauble, 2011; Macris *et al.*, 2013; Li *et al.*, 2016). 层状硅酸盐矿物和水溶液间也存在平衡镁同位素分馏, 其强 Mg-O 键导致硅酸盐矿物中相对富集重镁同位素 (Teng, 2017). 李伟强等 (2020) 发现斑岩铜矿中次生蚀变矿物与热液流体之间存在平衡 Mg 同位素分馏, 蚀变岩相对富集重镁同位素组成.

### 3.2 Mg 同位素动力学分馏

同位素的动力学效应可能与矿物表面的扩散运动以及质量对矿物—流体界面反应速率的依赖性有关(Watkins *et al.*, 2017). 镁同位素动力学分馏与其沿化学势和温度梯度的扩散有关(Richter *et al.*, 2008). 上升的熔体和围岩之间的镁同位素动力学分馏是产生轻镁同位素组成的潜在过程(Richter *et al.*, 2008; Huang and Xiao, 2016). 对碳酸岩浆而言, 其密度低粘度低, 可迅速上升, 碳酸岩岩浆中化学扩散和热扩散的时间都非常有限, 故其镁同位素动力学分馏不显著(Cheng *et al.*, 2017).

温度梯度引起的热扩散会使 Mg 同位素发生动力学同位素分馏, 使得较轻的同位素倾向于向热端扩散, 而较重的同位素则在冷端富集, 并最终进入玄武质熔岩或安山岩熔岩. 实验表明, 在 150 °C 温差下, 玄武岩熔体中冷端相对于热端可产生 8‰ 的镁同位素分馏(Richter *et al.*, 2008), 甚至达到 23‰(Huang *et al.*, 2010). 熔体中的热扩散比化学扩散快几个数量级, 很难长时间保持较大的温度梯度, 使得动力学同位素分馏难以长期保存. 目前, 自然地质样品中还没有发现由热扩散过程引起的显著镁同位素分馏(Yang *et al.*, 2009; 柯珊等, 2011; Teng, 2017; Guo *et al.*, 2019).

当系统中存在化学势梯度时, 会发生由化学扩散引起的动力学同位素分馏, 元素将从化学势的较高端扩散到较低端, 轻 Mg 同位素在扩散过程中的扩散速率比重 Mg 同位素快(扩散两端的 MgO 活度差越大, 镁同位素分馏效果越显著; 柯珊等, 2011). 实验模拟表明, 在玄武岩—流纹岩熔体中镁同位素分馏可达到 7‰(Richter *et al.*, 2008). 在达到扩散平衡之前, 可发生显著的由化学扩散引起的镁同位素动力学分馏. 化学扩散可以在大尺度上运移元素, 在共生矿物间、地质样品中、露头上均发现了化学扩散驱动的大规模镁同位素分馏(Teng *et al.*, 2011; Sio *et al.*, 2013; Xiao *et al.*, 2013; Oeser *et al.*, 2015; Pogge von Strandmann *et al.*, 2015; Hu *et al.*, 2016; Teng, 2017).

### 3.3 低温 Mg 同位素分馏

在化学风化过程中, 镁通过碳酸盐和硅酸盐的溶解而释放出来(Tipper *et al.*, 2012). 相对于高温地球化学过程而言, 表生环境(尤其是硅酸盐风化和碳酸盐沉淀过程)中的低温镁同位素分馏显著(Teng *et al.*, 2010b; 范百龄等, 2013; Lee *et al.*,

2014; Dessert *et al.*, 2015; 董爱国和朱祥坤, 2016; 董爱国和韩贵琳, 2017; Teng, 2017; Brewer *et al.*, 2018; Gao *et al.*, 2018; Fries *et al.*, 2019; Hindshaw *et al.*, 2019, 2020; Nitzsche *et al.*, 2019; Oskierski *et al.*, 2019; Tian *et al.*, 2019; Chen *et al.*, 2020a; Ryu *et al.*, 2021). Hindshaw *et al.* (2020) 研究表明, Mg 同位素分馏方向取决于晶格和溶液中 Mg-O 键长度的差异. 对海洋碎屑沉积物的镁同位素研究发现, 富碳酸盐沉积物富集轻 Mg 同位素而富粘土沉积物普遍富集重 Mg 同位素(Hu *et al.*, 2017b). 上地壳岩石经风化后, 一部分 Mg 以离子的形式进入水体, 或以次生矿物的形式留在原地(Liu *et al.*, 2014). 一般风成沉积物中硅酸盐的镁同位素组成与上地壳接近( $\delta^{26}\text{Mg} = -0.22\text{‰}$ ; 董爱国和朱祥坤, 2016). 而次生矿物(主要是粘土矿物)的 Mg 同位素组成变化较大, 其镁同位素组成特征与镁同位素在矿物晶格和矿物表面/层间的分馏有关(董爱国和朱祥坤, 2016). 相对水体而言, 风化或蚀变产生的次生层状硅酸盐矿物富集重的 Mg 同位素组成(Liu *et al.*, 2014; Teng, 2017; Gao *et al.*, 2018; 李伟强等, 2020; Ryu *et al.*, 2021), 这主要是因为层状硅酸盐矿物中 Mg-O 键的键能比水溶液中 Mg-O 键更强(Li *et al.*, 2014; Hindshaw *et al.*, 2020). 随着风化强度的增加, 镁同位素的分馏程度也呈现增加的趋势(Li *et al.*, 2010; 朱祥坤等, 2013).

碳酸盐岩的镁同位素组成显著轻于上地壳(董爱国和朱祥坤, 2016). 与其他碳酸盐岩相比, 白云岩富重镁(Geske *et al.*, 2015; Huang *et al.*, 2015c; Wang *et al.*, 2017c). 碳酸盐溶解和沉淀过程中, 镁同位素发生显著分馏, 碳酸盐矿物相对于溶液整体富集轻的镁同位素组成(Tipper *et al.*, 2006, 2008; Brenot *et al.*, 2008). 在沉淀过程中, 矿物类型是控制不同碳酸盐岩镁同位素组成的首要因素, 碳酸盐矿物与溶液的分馏程度如下:  $\Delta^{26}\text{Mg}_{\text{文石-水溶液}} \approx \Delta^{26}\text{Mg}_{\text{水合菱镁矿-水溶液}} < \Delta^{26}\text{Mg}_{\text{白云石-水溶液}} \approx \Delta^{26}\text{Mg}_{\text{菱镁矿-水溶液}} < \Delta^{26}\text{Mg}_{\text{方解石-水溶液}} < 0$ (董爱国和朱祥坤, 2016). 河流等水体的镁同位素组成与源岩有关, 源岩为硅酸盐的水体镁同位素组成比源岩轻, 源岩为碳酸盐的水体镁同位素组成比源岩略重, 但前者的镁同位素组成仍比后者的重(Tipper *et al.*, 2006; 董爱国和朱祥坤, 2016; 董爱国和韩贵琳, 2017). 在河流输送过程中, 镁同位素不发生分馏, 但河水的镁同位素组成易受外来物质输入(如风成沉积)等因素的影响(范

百龄等, 2013). 碳酸盐的沉淀是海水镁进入沉积岩的主要方式之一, 海水中的镁离子以沉积碳酸盐岩的方式在洋中脊发生水岩反应, 此过程重镁同位素倾向于进入岩石之中(董爱国和朱祥坤, 2016). 此外, 海水中的镁与黏土矿物的交换反应、洋壳低温蚀变反应等都会产生明显的镁同位素分馏(董爱国和朱祥坤, 2016; Huang *et al.*, 2018). 在此过程中, 黏土矿物倾向于吸附轻镁同位素, 而深海橄榄岩富集重 Mg 同位素(Liu *et al.*, 2017a).

## 4 Mg 同位素在碳酸岩研究中的应用

### 4.1 碳酸岩研究意义及存在的科学问题

稀土有工业“黄金”“维生素”之称, 在高科技、绿色能源、新能源汽车、航空航天和尖端武器等领域具有日益广泛的用途, 在国际战略资源中占有重要地位, 中国、美国、日本、欧盟均将稀土列入战略性新兴产业关键金属矿产名录(U. S. Geological Survey, 2018; 蒋少涌等, 2019; 王登红, 2019; 谢玉玲等, 2019, 2020; 翟明国等, 2019; 范宏瑞等, 2020; 侯增谦等, 2020). 很多超大型稀土(REE)矿床与碳酸岩和碱性岩有关, 集中分布在中国、美国、澳大利亚、巴西和越南等少数国家(蒋少涌等, 2019; 毛景文等, 2019; 翟明国等, 2019; 范宏瑞等, 2020). 这些碳酸岩型(包括碳酸岩及其杂岩体)REE 矿床是世界上最重要的 REE 矿床类型和最主要的 REE 来源, 贡献了世界稀土资源总量 99% 以上, 故备受矿床学家们关注(宋文磊等, 2013; Xie *et al.*, 2016, 2020; 刘琰等, 2017; U. S. Geological Survey, 2018). 在中国, 几乎所有轻稀土矿床都与碳酸岩有关, 贡献了中国稀土资源总量约 98%, 主要分布在内蒙、四川、山东、湖北、新疆、河南和陕西等地(谢玉玲等, 2019, 2020; Xie *et al.*, 2020). 然而, 值得注意的是, 世界上有超过 550 个碳酸岩体(Bell and Tilton, 2002; Woolley and Kjarsgaard, 2008; 谢玉玲等, 2019), 绝大部分碳酸岩高度富集 Sr、Ba 和 REE 元素( $100 \times 10^{-6} \sim 10\,000 \times 10^{-6}$ ; Castor, 2008; Bell and Simonetti, 2010), 但仅有部分碳酸岩(不超过 100 个)能形成大型或超大型 REE 矿床(谢玉玲等, 2019). 因此, 含矿碳酸岩成因及其源区稀土元素富集机制有待于进一步深入研究, 目前主要有 3 种观点: (1) 碳酸岩来自碳酸盐化地幔物质低程度的部分熔融, 该地幔源区受到富稀土元素大洋沉积物或壳源碳酸盐岩交代, 造成地幔源区富集稀土(Xu *et al.*, 2011,

2014; Hou *et al.*, 2015; Xie *et al.*, 2020); (2) 富  $\text{CO}_2$  幔源硅酸岩浆上侵过程中发生碳酸岩浆与硅酸岩浆的不混溶或者多相不混溶形成碳酸岩浆, 造成稀土元素在碳酸岩浆中富集(Wendlandt and Harrison, 1979; D' Orazio *et al.*, 1998; Zhang *et al.*, 2017); (3) 碳酸岩浆是富  $\text{CO}_2$  幔源硅酸岩浆经强烈的结晶分异形成, 结晶分异是造成残余碳酸岩浆稀土元素富集的主要机制(Twyman and Gittins, 1987; Doroshkevich *et al.*, 2017). 然而, 不同学者认为 REE 富集机制受多个过程控制. Su *et al.* (2019b) 和 Yang *et al.* (2019) 认为岩浆不混溶和分离结晶作用造成稀土元素在碳酸岩浆中富集, 分别形成了湖北庙垭 Nb-REE 矿床和内蒙白云鄂博 REE-Nb-Fe 矿床. 蒋少涌等(2019) 综述前人研究成果认为地幔源区、岩浆不混溶和分离结晶均造成了稀土元素富集.

Mg 同位素在高温岩浆过程中不发生有意义分馏, 原生岩浆 Mg 同位素组成可用来研究源区物质的组成(Li *et al.*, 2017; Liu *et al.*, 2017b; Teng, 2017; Tian *et al.*, 2019, 2020a, 2020b; Sun *et al.*, 2021a, 2021b). 不同类型沉积物的 Mg 同位素组成和含量差异明显, 比如, 富含粘土的陆源沉积物(Hu *et al.*, 2017b) 和低温蚀变洋壳(Huang *et al.*, 2015b, 2018) 具有相对重的  $\delta^{26}\text{Mg}$  值, 而沉积碳酸盐岩具有低的、变化范围大的  $\delta^{26}\text{Mg}$  ( $-5.6\% \sim -0.6\%$ ) 和 MgO 含量(高达 23%) (Saenger and Wang, 2014; Teng, 2017). 这些特性使 Mg 同位素体系成为良好的地球化学示踪工具, 在示踪岩浆碳酸岩岩浆源区和 REE 富集机制方面取得了重要进展. 比如, Ling *et al.* (2013) 发现白云鄂博方解石碳酸岩的  $\delta^{26}\text{Mg}$  为  $-2.28\% \sim -0.23\%$ , 认为俯冲板片富硅流体交代沉积碳酸盐岩造成稀土元素富集. Song *et al.* (2016) 发现秦岭碳酸岩的  $\delta^{26}\text{Mg}$  为  $-1.89\% \sim -1.07\%$ , 认为地幔源区中的循环沉积碳酸盐岩造成稀土元素富集. Cheng *et al.* (2017) 和 Song *et al.* (2017) 发现塔里木盆地大火成岩省碳酸岩的  $\delta^{26}\text{Mg}$  分别为  $-1.09\% \sim -0.85\%$  和  $-0.99\% \sim -0.65\%$ , 认为与循环碳酸盐岩有关. 下面比较详细地总结 Mg 同位素在碳酸岩 3 种成因观点研究方面的应用.

### 4.2 碳酸岩—硅酸盐液态不混溶和碳酸岩熔体分离结晶中的 Mg 同位素分馏

Li *et al.* (2016) 发现 Oldoinyo Lengai 橄榄石黄长岩  $\delta^{26}\text{Mg} = -0.30\% \sim -0.26\%$ , 与 MORB 和 OIB 的类似, 是由地幔低程度部分熔融形成的, 可能代



表示了该地区原生熔体. 橄榄石黄长岩具有类似地幔的 Mg 同位素组成, 表明在地幔部分熔融和橄榄石结晶过程中镁同位素分馏有限, 与前人的研究成果一致 (Teng *et al.*, 2007, 2010a; Bourdon *et al.*, 2010). 与硅酸盐-碳酸岩液态不混溶无关的高分异过碱性硅酸盐岩石 (Lengai I 响岩、Lengai II A 霞石岩和 2007—2008 年霞石岩) 的 MgO 含量变化范围较大 (2.0%~0.8%), 但  $\delta^{26}\text{Mg}$  变化范围很小 ( $-0.25\text{‰}\sim-0.10\text{‰}$ ; 图 3), 与地幔值类似, 说明在高度演化的过碱性硅酸盐岩浆结晶分异过程中镁同位素分馏很小 (图 3 中①所示). 而由硅酸盐-碳酸岩液态不混溶作用产生的 Lengai II B 霞石岩, 具有较重的 Mg 同位素组成 ( $-0.06\text{‰}\sim-0.09\text{‰}$ ; 图 3). 不同成因硅酸盐熔体的镁同位素组成差异表明硅酸盐-碳酸岩液态不混溶过程中产生了明显的镁同位素分馏, 硅酸盐熔体富集重镁同位素, 共生碳酸岩熔体则具有轻镁同位素组成 (图 3 中②所示). Li *et al.* (2016) 的研究成果佐证了 Schauble (2011) 和 Macris *et al.* (2013) 关于高温硅酸盐-碳酸盐矿物平衡镁同位素分馏的理论计算和实验模拟结果: 重镁同位素相对于碳酸岩熔体优先分配到硅酸盐熔体. 因此, 原始碳酸岩熔体应该具有轻的  $\delta^{26}\text{Mg}$  (图 3), 而 Oldoinyo Lengai 钠质碳酸岩  $\delta^{26}\text{Mg}$  为  $0.13\text{‰}\sim 0.37\text{‰}$  (图 3), 远高于原始地幔值, 表明在液态不混溶之后, 碳酸岩熔体发生了分离结晶作用, 造成分异的碳酸盐矿物具有轻的  $\delta^{26}\text{Mg}$ , 而残余熔体富集重的  $\delta^{26}\text{Mg}$ . 如图 4 所示, 钠质碳酸岩  $\delta^{26}\text{Mg}$  与碱金属 ( $\text{Na}_2\text{O}+\text{K}_2\text{O}$ ) 和碱土金属 ( $\text{CaO}+\text{SrO}+\text{BaO}$ ) 呈负相关关系, 表明碳酸岩熔体结晶分异 (菱钠钙石和钛铁矿的分离结晶) 过程会发生 Mg 同位素分馏, 重 Mg 同位素倾向于在残余碳酸岩熔体中富集 (图 3 中③所示, 图 4). 因此, 菱钠钙石和钛铁矿这两种富含碱金属和碱土金属矿物的分离结晶可能是导致钠质碳酸岩镁同位素组成向重同位素变化的原因. 因此, 在碳酸岩-硅酸盐液态不混溶和碳酸岩熔体分离结晶过程中均发生了明显的镁同位素分馏, 对碳酸岩岩石成因有关的这两种作用来说, 镁同位素是一种潜在有用的示踪剂.

#### 4.3 Mg 同位素可识别碳酸岩源区中的再循环沉积碳酸盐岩

Ling *et al.* (2013) 发现方解石碳酸岩的  $\delta^{26}\text{Mg}$  值 ( $-2.28\text{‰}\sim 0.23\text{‰}$ ) 不同于含矿白云岩 ( $-0.67\text{‰}\sim 0.28\text{‰}$ ) 和白云石碳酸岩 ( $\delta^{26}\text{Mg} = -0.20\text{‰}\sim$

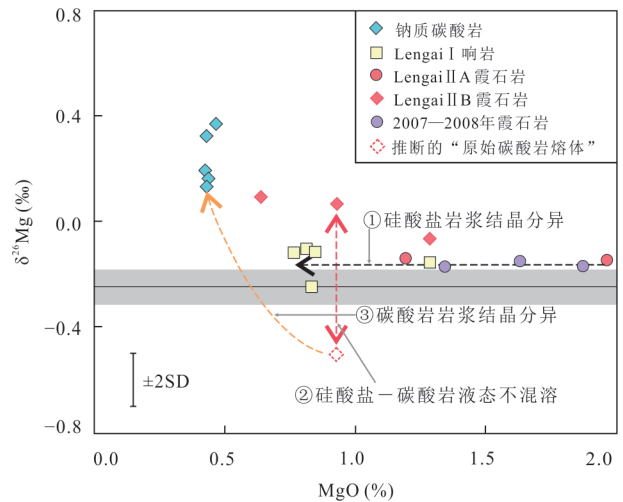


图 3 Oldoinyo Lengai 过碱性硅酸盐和钠质碳酸岩  $\delta^{26}\text{Mg}$  与 MgO 关系图解 (据 Li *et al.*, 2016)

Fig. 3  $\delta^{26}\text{Mg}$  with MgO for peralkaline silicate rocks and natrocarbonatites from Oldoinyo Lengai (after Li *et al.*, 2016)

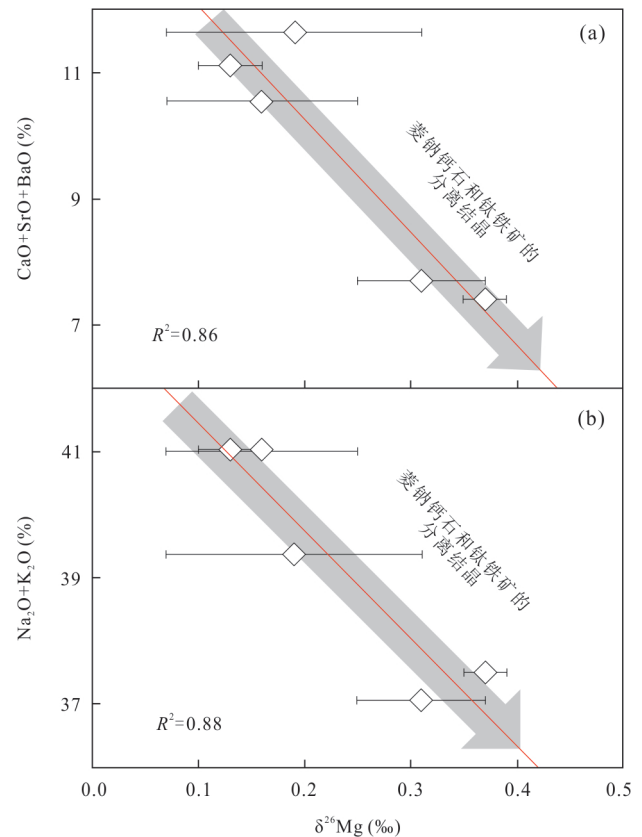


图 4 Oldoinyo Lengai 钠质碳酸岩  $\delta^{26}\text{Mg}$  与  $\text{CaO}+\text{SrO}+\text{BaO}$  (a) 和  $\text{Na}_2\text{O}+\text{K}_2\text{O}$  (b) 的关系图解 (据 Li *et al.*, 2016)

Fig. 4  $\delta^{26}\text{Mg}$  with  $\text{CaO}+\text{SrO}+\text{BaO}$  (a) and  $\text{Na}_2\text{O}+\text{K}_2\text{O}$  (b) for natrocarbonatites from Oldoinyo Lengai (after Li *et al.*, 2016)

-0.46‰) 的  $\delta^{26}\text{Mg}$  值. 大部分含矿白云岩的 Mg 同位素组成可以用幔源物质 ( $-0.25\text{‰} \pm 0.07\text{‰}$ ; Teng *et al.*, 2010a) 与方解石碳酸岩的混合来解释. 镁同位素含量、C-O 同位素特征、主微量元素和 Th/U、Nb/U、Th/Nb、Ce/Lu 等表明稀土矿体与白云石碳酸岩具有相似的地球化学特征. 方解石碳酸岩分为两组: 低  $\text{SiO}_2$  和 MgO 含量的样品具有低  $\delta^{26}\text{Mg}$  值, 而高  $\text{SiO}_2$  和 MgO 含量的样品具有类似地幔的  $\delta^{26}\text{Mg}$  值, 表明有  $\text{SiO}_2$  和 MgO 的加入 (图 5). 部分方解石碳酸岩样品位于地幔与具有最低 Mg 含量和  $\delta^{26}\text{Mg}$  值的方解石碳酸岩样品之间的混合线上 (图 5b). 据此, Ling *et al.* (2013) 认为方解石碳酸岩与俯冲板片释放的具有地幔镁同位素组成的富 Si 流体发生了反应, 淋滤出了 REE, 含矿流体继续运移交代沉积碳酸盐岩造成了稀土元素的富集, 最终形成了白云鄂博巨型稀土矿床. Song *et al.* (2016) 发现南秦岭和北秦岭富 REE 碳酸岩的  $\delta^{26}\text{Mg}$  ( $-1.89\text{‰} \sim -1.07\text{‰}$ ) 明显低于典型的幔源岩石 ( $-0.25\text{‰} \pm 0.07\text{‰}$ ; Teng *et al.*, 2010a), 也不同于裂谷环境碳酸岩 ( $0.13\text{‰} \sim 0.37\text{‰}$ ; Li *et al.*, 2016), 而近似于海相白云岩 ( $-2.5\text{‰} \sim -1.0\text{‰}$ ; Huang *et al.*, 2015c). 在地幔熔融、橄榄石和辉石结晶等过程中镁同位素分馏很小 (Teng *et al.*, 2010a; Macris *et al.*, 2013; Li *et al.*, 2016), 而碳酸岩熔体中碳酸盐矿物的结晶分异 (Li *et al.*, 2016) 以及中下地壳 ( $-0.26\text{‰} \sim -0.21\text{‰}$ ; Yang *et al.*, 2016) 和上地壳 ( $-0.52\text{‰} \sim 0.92\text{‰}$ ; Li *et al.*, 2010) 混染将提高幔源岩浆的 Mg 同位素组成. 据此, Song *et al.* (2016) 推测秦岭碳酸

岩的地幔源区含有循环沉积碳酸盐岩, 由此造成了稀土元素的富集.

Cheng *et al.* (2017) 发现塔里木大火成岩省瓦吉里塔格镁质碳酸岩具有轻镁同位素值 ( $\delta^{26}\text{Mg} = -1.09\text{‰} \sim -0.85\text{‰}$ ). 尽管如前所述, 碳酸岩-硅酸盐液态不混溶和碳酸岩熔体分离结晶中存在 Mg 同位素分馏, 但岩相学研究表明瓦吉里塔格镁质碳酸岩的轻镁同位素值与富  $\text{CO}_2$  的硅酸盐熔体液态不混溶无关 (Cheng *et al.*, 2017). 富  $\text{CO}_2$  硅酸盐岩浆的结晶分异作用会产生大量镁铁质硅酸盐矿物 (橄榄石、斜方辉石、金云母、角闪石) 的分离结晶, 导致残余碳酸岩岩浆贫 Mg, 因此, 瓦吉里塔格镁质碳酸岩的高 MgO 含量表明其成因与富  $\text{CO}_2$  硅酸盐岩浆的分离结晶无关 (Cheng *et al.*, 2017). 瓦吉里塔格镁质碳酸岩  $\delta^{26}\text{Mg}$  与主要氧化物 MgO、CaO、 $\text{TFe}_2\text{O}_3$ 、 $\text{P}_2\text{O}_5$  和不相容元素 La、Sr 无相关性, 表明白云石、方解石、霓石、独居石和磷灰石的分离结晶对镁质碳酸岩 Mg 同位素的影响可忽略不计 (图 6). 根据岩相学观察, Cheng *et al.* (2017) 也排除了菱钠钙石和钛铁矿的分离结晶对瓦吉里塔格镁质碳酸岩镁同位素组成的影响. 前人研究也表明硅酸盐岩浆作用过程中镁同位素分馏不明显以及镁铁质硅酸盐矿物的分离结晶不产生明显的镁同位素分馏 (小于  $\pm 0.07\text{‰}$ ; Teng *et al.*, 2007, 2010a; Li *et al.*, 2010), 不可能导致瓦吉里塔格镁质碳酸岩产生极低的轻 Mg 同位素组成 ( $\delta^{26}\text{Mg} = -1.09\text{‰} \sim -0.85\text{‰}$ ). 因此, 瓦吉里塔格镁质碳酸岩与富  $\text{CO}_2$  饱和和硅酸盐熔体的液态不混溶和分离结晶无关, 而与再循环碳酸盐岩有

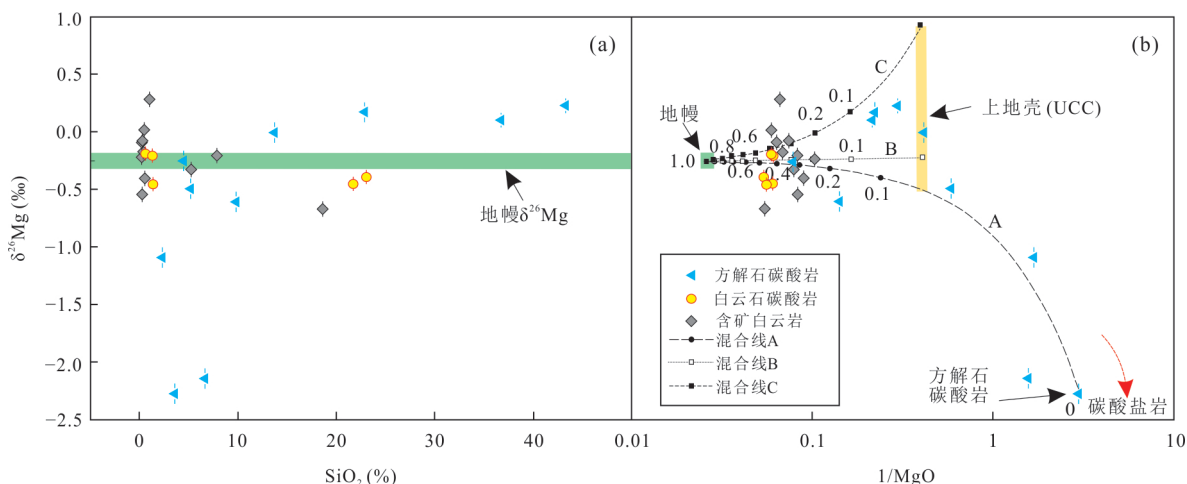


图 5 白云鄂博矿床方解石和白云石碳酸岩和含矿白云岩  $\delta^{26}\text{Mg}$  与  $\text{SiO}_2$  (a) 和  $1/\text{MgO}$  (b) 关系图解 (据 Ling *et al.*, 2013)

Fig. 5  $\delta^{26}\text{Mg}$  with  $\text{SiO}_2$  (a) and  $1/\text{MgO}$  (b) for calcitic and dolomitic carbonatites and ore-bearing dolomites in the Bayan E'bo deposit (after Ling *et al.*, 2013)

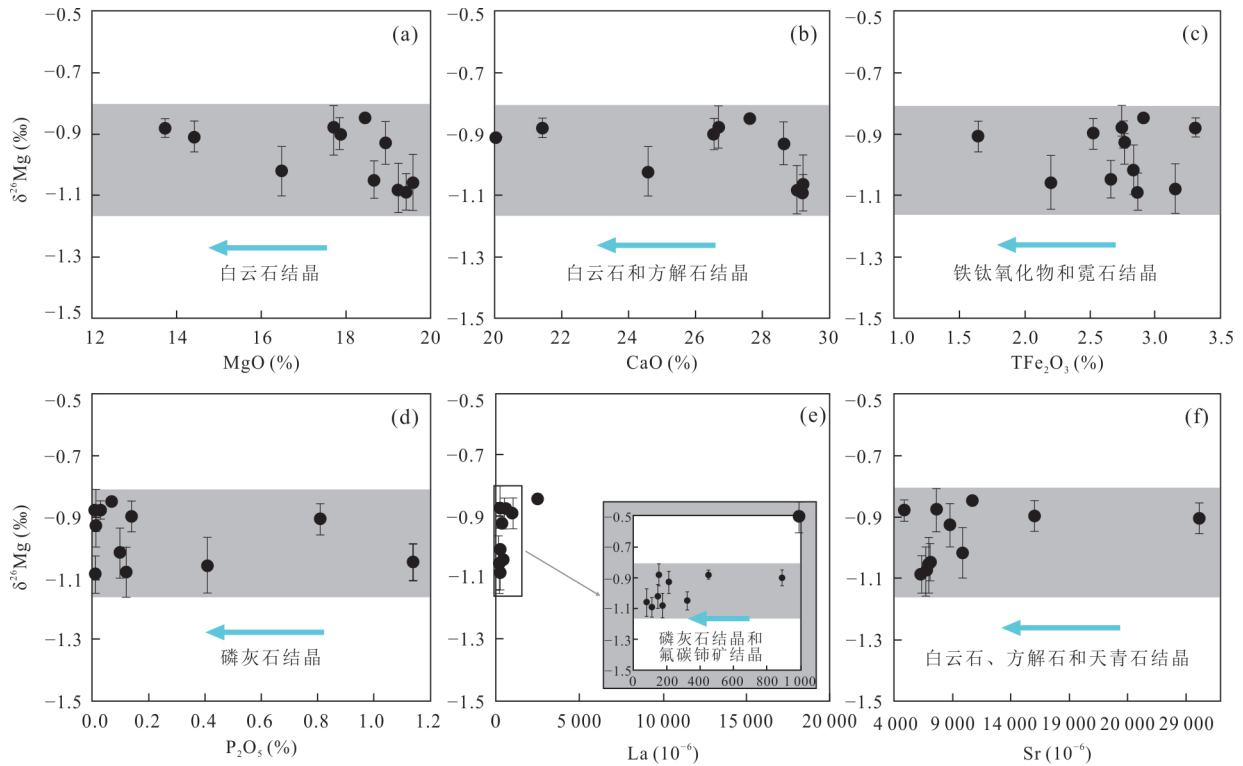


图 6 瓦吉里塔格镁质碳酸岩  $\delta^{26}\text{Mg}$  与  $\text{MgO}$ (a)、 $\text{CaO}$ (b)、 $\text{TFe}_2\text{O}_3$ (c)、 $\text{P}_2\text{O}_5$ (d)、 $\text{La}$ (e)和  $\text{Sr}$ (f)关系图解(据 Cheng *et al.*, 2017)  
 Fig.6 Variations of  $\delta^{26}\text{Mg}$  with the  $\text{MgO}$  (a),  $\text{CaO}$  (b),  $\text{TFe}_2\text{O}_3$  (c),  $\text{P}_2\text{O}_5$  (d),  $\text{La}$  (e) and  $\text{Sr}$  (f) in the Wajilitage magnesiocarbonatites (after Cheng *et al.*, 2017)

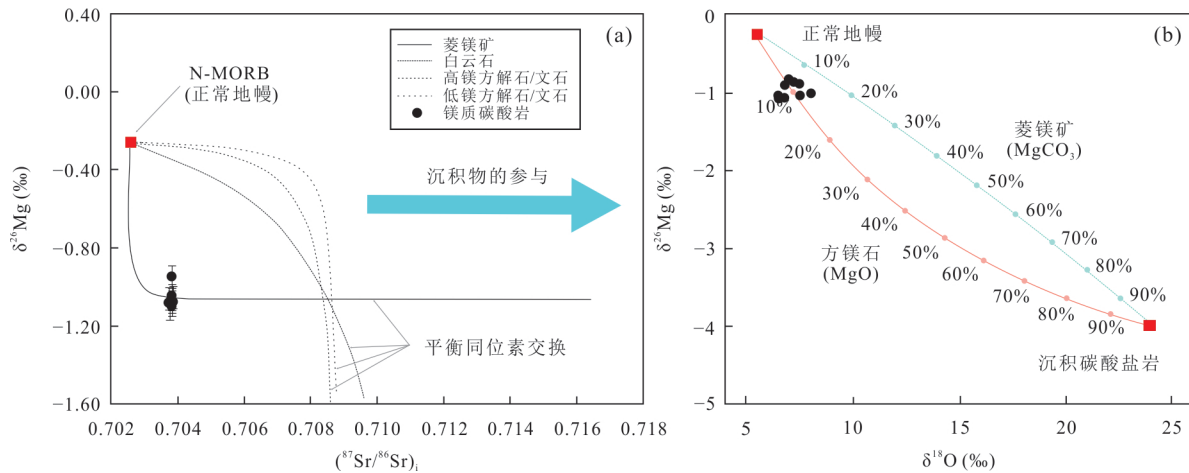


图 7 N-MORB 与菱镁矿、白云石和方解石/文石间 Mg 和 Sr 同位素交换模型(a), 正常地幔和沉积碳酸盐岩间的 Mg 和 O 同位素混合模型(b)

Fig.7 Mg and Sr isotope exchange model between N-MORB and magnesite, dolomite and calcite/aragonite (a) and Mg and O isotopic mix modeling between the normal mantle and sedimentary carbonates (b)

a 据 Wang *et al.* (2016b)和 Cheng *et al.* (2017); b 据 Cheng *et al.* (2017)

关(Cheng *et al.*, 2017).再循环碳酸盐(方解石/白云石)首先在俯冲浅部相变为菱镁矿( $\text{MgCO}_3$ )并生成透辉石.Sr和Ca通过类质同象共存并优先进入透辉石等硅酸盐矿物,导致再循环碳酸盐中Sr含量急剧

下降.Mg和Sr同位素的解耦可通过N-MORB(正常地幔)和菱镁矿之间的Mg-Sr交换模型来解释(图7a; Wang *et al.*, 2016b; Cheng *et al.*, 2017),这与瓦吉里塔格镁质碳酸岩具有地幔的Sr同位素特征一

致 ( $^{87}\text{Sr}/^{86}\text{Sr}$ )<sub>i</sub> = 0.703 78~0.703 86; Cheng *et al.*, 2017). 随着下沉深度的增加, 板块俯冲至地幔深处最终由菱镁矿相变为镁钙钛矿/方镁石和碳 (Mg-SiO<sub>3</sub>/MgO+C) 的组合物并释放出 CO<sub>2</sub> (Seto *et al.*, 2008; Solopova *et al.*, 2015) 和 O<sub>2</sub> (Litasov *et al.*, 2011). 碳酸盐矿物中的氧被释放出来导致没有足够的再循环氧来改变瓦吉里塔格镁质碳酸岩的 O 同位素组成, 这与其具有地幔的氧同位素特征一致 ( $\delta^{18}\text{O}_{\text{V-SMOW}} = 5.9\text{‰} \sim 8.0\text{‰}$ ; Cheng *et al.*, 2017). 随着地幔柱上升, C 在 60~150 km 处会以 CO<sub>2</sub> 或碳酸盐的形式被氧化, 导致固相线下降并诱导地幔橄榄岩发生熔融生成碳酸岩 (Taylor and Green, 1988; Hammouda and Keshav, 2015). Cheng *et al.* (2017) 根据地幔和沉积碳酸盐的 Mg 和 O 同位素组成, 通过含方镁石和菱镁矿的原始地幔和碳酸盐岩的二元混合模拟碳酸盐交代作用的过程, 推断出约 10% 的再循环碳酸盐岩混入了瓦吉里塔格镁质碳酸岩的地幔源岩中 (图 7b). Song *et al.* (2017) 报告了该地的另一组镁质碳酸岩的  $\delta^{26}\text{Mg}$  值 ( $-0.99\text{‰} \sim -0.65\text{‰}$ ) 也与循环碳酸盐有关, 认为碳酸岩是循环沉积物与地幔橄榄岩混合减压、熔融形成的.

## 5 其他有关问题的探讨

### 5.1 幔源岩石低 $\delta^{26}\text{Mg}$ 成因解释

(1) 与俯冲再循环的碳酸盐岩或洋壳物质有关: 华南和东北玄武岩、拉萨地块超钾质火山岩、新疆正长岩和韩国济州岛碱性火山岩均具有低  $\delta^{26}\text{Mg}$  值, 认为其地幔源区含有再循环的碳酸盐岩 (Yang *et al.*, 2012; Huang *et al.*, 2015a; Liu *et al.*, 2015; Ke *et al.*, 2016; Tian *et al.*, 2016; Wang *et al.*, 2017b; Kim *et al.*, 2019). 然而, Wang *et al.* (2016a) 和 Sun *et al.* (2017) 发现玄武岩或火山岩具有低  $\delta^{26}\text{Mg}$  值, 且与 (Gd/Yb)<sub>N</sub> 或 TiO<sub>2</sub> 呈负相关, 认为其地幔源区含有再循环的洋壳物质 (碳酸盐化榴辉岩). Li *et al.* (2017) 认为中国东部地幔存在两个不同成因的低  $\delta^{26}\text{Mg}$  同位素异常区: ① 东部大陆上地幔低  $\delta^{26}\text{Mg}$  同位素异常区, 是沉积碳酸盐岩再循环形成的; ② 海南低  $\delta^{26}\text{Mg}$  同位素异常区, 是再循环洋壳物质以碳酸盐化榴辉岩形式加入地幔源区造成的. 区分洋壳物质 (碳酸盐化榴辉岩) 和碳酸盐岩, 主要有 3 种方式: ① 判断洋壳俯冲深度, 形成榴辉岩俯冲深度大于 120 km (Ringwood, 1990); ②  $\delta^{26}\text{Mg}$  与 Fe/Mn、CaO/Al<sub>2</sub>O<sub>3</sub>、Gd/Yb、TiO<sub>2</sub> 相关性 (Wang *et al.*,

2016a; Li *et al.*, 2017; Sun *et al.*, 2017); ③ 碳酸盐岩交代形成的熔体具有低 Fe/Mn、Hf/Hf、Ti/Ti<sup>+</sup> 和高 CaO/Al<sub>2</sub>O<sub>3</sub> 比值, 而洋壳物质交代形成的熔体则相反 (Li *et al.*, 2017).

(2) 与矿物分离结晶有关: Su *et al.* (2019a) 认为玄武质熔体上升过程中由于铬铁矿的结晶分异造成熔体的轻  $\delta^{26}\text{Mg}$  特征, 这是因为铬铁矿具有相对重的 Mg 同位素组成. 铬铁矿是玄武岩岩浆中的早期结晶相, 比硅酸盐矿物富镁 (MgO > 10%), 具有更重的镁同位素组成 ( $\delta^{26}\text{Mg} = -0.10\text{‰} \sim -0.40\text{‰}$ ; Xiao *et al.*, 2016; Su *et al.*, 2017a).  $\delta^{26}\text{Mg}$  与玄武岩中 Cr、V、Fe、Ti 含量的相关性强烈表明, 演化岩浆的镁同位素组成越来越轻与铬铁矿的分离结晶有关. 铬铁矿-熔体模拟结果表明最大 7% 和 4% 的铬铁矿结晶可导致玄武岩产生轻镁同位素异常 (图 8; 红色和蓝色实线代表计算出的残余熔体 Mg 同位素组成). Wang *et al.* (2021) 发现高分异玄武岩的  $\delta^{26}\text{Mg}$  为  $-0.36\text{‰} \sim -0.14\text{‰}$ , 认为是由重镁同位素组成的钛磁铁矿和轻镁同位素组成的钛铁矿分离结晶所致. 钛磁铁矿的  $\delta^{26}\text{Mg}$  (0.15%~0.52%) 值明显高于全岩 ( $-0.14\text{‰} \sim -0.36\text{‰}$ )、橄榄石 ( $-0.36\text{‰} \sim -0.30\text{‰}$ ) 和单斜辉石 ( $-0.33\text{‰} \sim -0.29\text{‰}$ ) 的  $\delta^{26}\text{Mg}$  值, 富重镁同位素的钛磁铁矿分离结晶会促使残余岩浆逐渐富集轻的 Mg 同位素组成. 镁同位素分馏定量模拟表明  $\Delta^{26}\text{Mg}_{\text{钛磁铁矿-熔体}}$  为正,  $\Delta^{26}\text{Mg}_{\text{钛铁矿-熔体}}$  为负, 钛磁铁矿的分离结晶会降低氧含量, 有利于后期钛铁矿的分离结晶, 使  $\delta^{26}\text{Mg}$ -MgO 的相关性由正变负 (Wang *et al.*, 2021).

### 5.2 Li-Mg-Ca 同位素联合示踪岩浆碳酸岩岩石成因

Li、Mg、Ca 同位素在示踪同一地区或不同时代的碳酸岩岩石成因方面, 存在多种观点. 比如, 对于坦桑尼亚 Oldoinyo Lengai 钠质碳酸岩: Halama *et al.* (2007) 发现该套钠质碳酸岩  $\delta^7\text{Li}$  为 3.3%~5.1%, 与 MORB 和 OIB 的类似, 而与碳酸岩液态不混溶有关的高分异过碱性霞石岩的  $\delta^7\text{Li}$  为 3.0%, 与碳酸岩的类似, 表明在碳酸岩-硅酸盐液态不混溶过程中没有发生明显的 Li 同位素分馏, 其源区未受碳酸盐岩交代; Li *et al.* (2016) 发现该套钠质碳酸岩  $\delta^{26}\text{Mg}$  为 0.13%~0.37%, 而与碳酸岩液态不混溶有关的高分异霞石岩的  $\delta^{26}\text{Mg}$  为  $-0.06\text{‰} \sim 0.09\text{‰}$ , 表明在液态不混溶之后, 碳酸岩熔体发生了分离结晶作用, 造成分异的碳酸盐矿物具有轻的  $\delta^{26}\text{Mg}$ , 而残

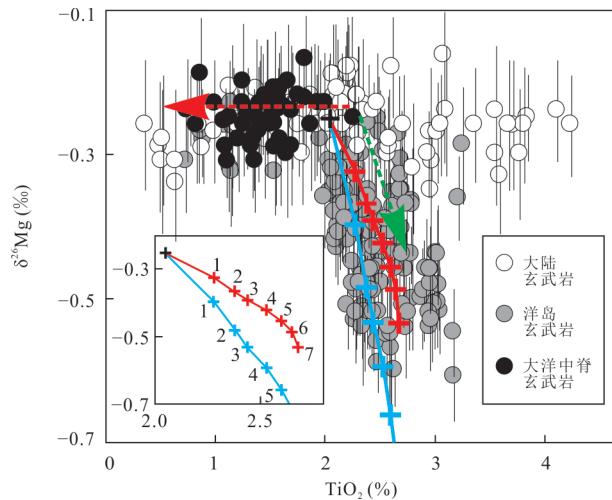


图 8 玄武岩  $\delta^{26}\text{Mg}$  与  $\text{TiO}_2$  关系图解(据 Su *et al.*, 2019a)

Fig.8  $\delta^{26}\text{Mg}$  vs.  $\text{TiO}_2$  contents of the basalts (after Su *et al.*, 2019a)

余熔体富集重的  $\delta^{26}\text{Mg}$ . 在碳酸岩—硅酸盐液态不混溶和碳酸岩熔体分离结晶过程中均发生了明显的镁同位素分馏; Amsellem *et al.* (2020) 发现该套钠质碳酸岩平均 Ca 同位素组成  $\delta^{44/40}\text{Ca}$  为  $0.71\text{‰} \pm 0.20\text{‰}$ , 认为钠质碳酸岩是通过霞石岩浆液态不混溶形成的, 其源区未受碳酸盐岩交代.

又如, 对于不同时代的碳酸岩和硅酸盐 Halama *et al.* (2008) 发现这些岩石具有类似的  $\delta^7\text{Li}$  值, 为  $1\text{‰} \sim 7\text{‰}$ , 与地幔柱有关, 没有受到俯冲作用和地壳循环的影响; Amsellem *et al.* (2020) 发现碳酸岩(除 Oldoinyo Lengai 碳酸岩外)  $\delta^{44/40}\text{Ca}$  为  $0.26\text{‰} \pm 0.25\text{‰}$ , 认为其地幔源区含  $7\%$  碳酸盐岩; Sun *et al.* (2021c) 发现碳酸岩和硅酸盐  $\delta^{44/42}\text{Ca}$  为  $0.35\text{‰} \pm 0.01\text{‰}$ , 与全球范围的玄武岩相近(平均  $\delta^{44/42}\text{Ca} = 0.37\text{‰} \pm 0.01\text{‰}$ ), 认为来自正常幔源, 源区不需要循环碳酸盐的任何贡献; Banerjee *et al.* (2021) 发现大于 300 Ma 碳酸岩的  $\delta^{44/40}\text{Ca}$  与地幔值类似, 而小于 300 Ma 碳酸岩的  $\delta^{44/40}\text{Ca}$  值比地幔值轻, 认为其地幔源区含小于  $10\%$  碳酸盐岩.

正如 Liu and Li (2019) 和向蜜等 (2021) 强调利用多种金属同位素联合示踪来探讨岩石成因一样, 本文也认为有必要通过 Li-Mg-Ca 同位素联合示踪来识别岩浆碳酸岩的源区特征和交代富集组分, 阐明深部岩浆过程和动力学过程间的耦合关系, 进而揭示岩浆源区稀土元素超常富集机制, 完善碳酸岩型稀土矿床成矿模型, 实现稀土成矿理论突破, 为稀土资源找矿勘查提供理论依据.

## 6 总结与展望

(1) Mg 同位素高达  $8.33\text{‰}$  的质量差使得其在各种地质过程中能够发生明显的同位素质量分馏,  $\delta^{26}\text{Mg}$  变化高达  $7.0\text{‰}$ , 具有重要的示踪潜力. 高精度的 Mg 同位素测定是进行 Mg 同位素地质应用的前提, 随着 MC-ICP-MS 的 Mg 同位素测定方法的优化, Mg 同位素在低温风化作用、高温部分熔融与岩浆结晶分异、变质作用、板片俯冲及壳幔物质循环、热液蚀变和矿床成因等方面展现出了其广阔的应用前景. 随着同位素测定技术的创新和改进, 2017 年 Nu 仪器推出一款全新的碰撞反应池多接收器电感耦合等离子体质谱仪 (Nu Sapphire MC-ICP-MS), 该仪器拥有一个高能量通道, 同时拥有一个低能量通道, 引导离子束通过六极杆碰撞池, 去除 ICP 产生的与 Mg、Si、S、K、Ca、Ti、V、Cr、Fe、Ni 和 Se 等金属同位素有相同质量数的多原子干扰物, 使得在低分辨率模式下对这些同位素体系进行分析成为可能, 保持了原有的离子传输效率, 并显著降低样品使用量, 将同位素分析的精度和准确度提升至计数统计学水平. 目前, 使用该仪器分析了 K 同位素组成 (Ku and Jacobsen, 2020; Moynier *et al.*, 2021a, 2021b), 显示出了巨大的分析优势, 相信能对金属同位素的发展带来技术上的革命, 从而为解决地质演化和地球动力学研究中的关键科学问题提供新的技术手段.

(2) Mg 同位素在碳酸岩中的应用研究仍存在尚未解决的科学问题. 一是幔源岩石低  $\delta^{26}\text{Mg}$  成因存在争议, 有研究认为其与俯冲再循环的碳酸盐岩或洋壳物质有关, 也有观点指出矿物分离结晶导致了  $\delta^{26}\text{Mg}$  异常, 地幔镁同位素不均匀性的成因有待进一步研究; 二是含 REE 矿碳酸岩成因及其源区稀土元素富集机制尚不明确. Mg 同位素体系可作为地球化学示踪工具参与岩浆碳酸岩岩浆源区示踪和 REE 富集机制探索, 但单一同位素示踪有其局限性, 有必要开展 Li-Mg-Ca 同位素联合示踪岩浆碳酸岩岩石成因. 如前所述, 中国几乎所有的轻稀土矿床都与碳酸岩有关, 贡献了中国稀土资源总量约  $98\%$ , 然而含矿碳酸岩成因及其源区稀土元素富集机制有待进一步深入研究. 有鉴于此, 国家自然科学基金委员会于 2019 年 7 月启动了“战略性关键金属超常富集成矿动力学”重大研究计划; 2021 年, 国家重点研发计划也启动实施“战略性矿产资源开发

利用”重点专项,将碳酸岩型稀土矿床超常富集机制研究作为其中的一部分研究内容.本文系统总结了镁同位素在碳酸岩研究中的应用、幔源岩石低 $\delta^{26}\text{Mg}$ 成因解释和Li-Mg-Ca同位素联合示踪岩浆碳酸岩岩石成因.为此,笔者相信可通过Li-Mg-Ca等金属同位素联合示踪,识别不同类型碳酸岩的岩浆源区特征、岩浆演化过程和交代富集组分,进而揭示稀土元素超常富集机制,完善碳酸岩型稀土矿床成矿模型,实现稀土矿床成矿理论突破,为稀土资源找矿勘查提供理论依据.

## References

- Amsellem, E., Moynier, F., Bertrand, H., et al., 2020. Calcium Isotopic Evidence for the Mantle Sources of Carbonatites. *Science Advances*, 6(23): eaba3269. <https://doi.org/10.1126/sciadv.aba3269>
- An, Y. J., Huang, J. X., Griffin, W. L., et al., 2017. Isotopic Composition of Mg and Fe in Garnet Peridotites from the Kaapvaal and Siberian Cratons. *Geochimica et Cosmochimica Acta*, 200: 167–185. <https://doi.org/10.1016/j.gca.2016.11.041>
- An, Y. J., Wu, F., Xiang, Y. X., et al., 2014. High-Precision Mg Isotope Analyses of Low-Mg Rocks by MC-ICP-MS. *Chemical Geology*, 390: 9–21. <https://doi.org/10.1016/j.chemgeo.2014.09.014>
- Antonelli, M. A., Simon, J. I., 2020. Calcium Isotopes in High-Temperature Terrestrial Processes. *Chemical Geology*, 548: 119651. <https://doi.org/10.1016/j.chemgeo.2020.119651>
- Bai, Y., Su, B. X., Xiao, Y., et al., 2021. Magnesium and Iron Isotopic Evidence of Inter-Mineral Diffusion in Ultramafic Cumulates of the Peridotite Zone, Stillwater Complex. *Geochimica et Cosmochimica Acta*, 292: 152–169. <https://doi.org/10.1016/j.gca.2020.09.023>
- Banerjee, A., Chakrabarti, R., Simonetti, A., 2021. Temporal Evolution of  $\delta^{44/40}\text{Ca}$  and  $^{87}\text{Sr}/^{86}\text{Sr}$  of Carbonatites: Implications for Crustal Recycling through Time. *Geochimica et Cosmochimica Acta*, 307: 168–191. <https://doi.org/10.1016/j.gca.2021.05.046>
- Bao, Z. A., Zong, C. L., Chen, K. Y., et al., 2020. Chromatographic Purification of Ca and Mg from Biological and Geological Samples for Isotope Analysis by MC-ICP-MS. *International Journal of Mass Spectrometry*, 448: 116268. <https://doi.org/10.1016/j.ijms.2019.116268>
- Bell, K., Simonetti, A., 2010. Source of Parental Melts to Carbonatites—Critical Isotopic Constraints. *Mineralogy and Petrology*, 98(1–4): 77–89. <https://doi.org/10.1007/s00710-009-0059-0>
- Bell, K., Tilton, G. R., 2002. Probing the Mantle: The Story from Carbonatites. *EOS, Transactions American Geophysical Union*, 83(25): 273–277. <https://doi.org/10.1029/2002eo000190>
- Bialik, O. M., Wang, X. M., Zhao, S. G., et al., 2018. Mg Isotope Response to Dolomitization in Hinterland-Attached Carbonate Platforms: Outlook of  $\delta^{26}\text{Mg}$  as a Tracer of Basin Restriction and Seawater Mg/Ca Ratio. *Geochimica et Cosmochimica Acta*, 235: 189–207. <https://doi.org/10.1016/j.gca.2018.05.024>
- Bolou-Bi, E. B., Vigier, N., Brenot, A., et al., 2009. Magnesium Isotope Compositions of Natural Reference Materials. *Geostandards and Geoanalytical Research*, 33(1): 95–109. <https://doi.org/10.1111/j.1751-908X.2009.00884.x>
- Bourdon, B., Tipper, E. T., Fitoussi, C., et al., 2010. Chondritic Mg Isotope Composition of the Earth. *Geochimica et Cosmochimica Acta*, 74(17): 5069–5083. <https://doi.org/10.1016/j.gca.2010.06.008>
- Brenot, A., Cloquet, C., Vigier, N., et al., 2008. Magnesium Isotope Systematics of the Lithologically Varied Moselle River Basin, France. *Geochimica et Cosmochimica Acta*, 72(20): 5070–5089. <https://doi.org/10.1016/j.gca.2008.07.027>
- Brewer, A., Teng, F. Z., Dethier, D., 2018. Magnesium Isotope Fractionation during Granite Weathering. *Chemical Geology*, 501: 95–103. <https://doi.org/10.1016/j.chemgeo.2018.10.013>
- Castor, S. B., 2008. The Mountain Pass Rare-Earth Carbonatite and Associated Ultrapotassic Rocks, California. *The Canadian Mineralogist*, 46(4): 779–806. <https://doi.org/10.3749/canmin.46.4.779>
- Chakrabarti, R., Jacobsen, S. B., 2010. The Isotopic Composition of Magnesium in the Inner Solar System. *Earth and Planetary Science Letters*, 293(3–4): 349–358. <https://doi.org/10.1016/j.epsl.2010.03.001>
- Chang, V. T. C., Makishima, A., Belshaw, N. S., et al., 2003. Purification of Mg from Low-Mg Biogenic Carbonates for Isotope Ratio Determination Using Multiple Collector ICP-MS. *Journal of Analytical Atomic Spectrometry*, 18(4): 296–301. <https://doi.org/10.1039/b210977h>
- Chaussidon, M., Deng, Z. B., Villeneuve, J., et al., 2017. In Situ Analysis of Non-Traditional Isotopes by SIMS and LA-MC-ICP-MS: Key Aspects and the Example of Mg Isotopes in Olivines and Silicate Glasses. *Reviews in Mineralogy and Geochemistry*, 82(1): 127–163. <https://doi.org/10.2138/rmg.2017.82.5>
- Chen, C. F., Huang, J. X., Foley, S. F., et al., 2020b. Composi-

- tional and Pressure Controls on Calcium and Magnesium Isotope Fractionation in Magmatic Systems. *Geochimica et Cosmochimica Acta*, 290: 257–270. <https://doi.org/10.1016/j.gca.2020.09.006>
- Chen, X. Y., Teng, F. Z., Huang, K. J., et al., 2020a. Intensified Chemical Weathering during Early Triassic Revealed by Magnesium Isotopes. *Geochimica et Cosmochimica Acta*, 287: 263–276. <https://doi.org/10.1016/j.gca.2020.02.035>
- Chen, Y. X., 2019. Reversed Metasomatism at the Slab-Mantle Interface in a Continental Subduction Channel: Geochemical Evidence from the Ultrahigh-Pressure Metamorphic Whiteschist in the Western Alps. *Earth Science*, 44(12): 4057–4063 (in Chinese with English abstract). <https://doi.org/10.3799/dqkx.2019.241>
- Chen, Y. X., Demény, A., Schertl, H. P., et al., 2020c. Tracing Subduction Zone Fluids with Distinct Mg Isotope Compositions: Insights from High-Pressure Metasomatic Rocks (Leucophyllites) from the Eastern Alps. *Geochimica et Cosmochimica Acta*, 271: 154–178. <https://doi.org/10.1016/j.gca.2019.12.025>
- Cheng, Z. G., Zhang, Z. C., Hou, T., et al., 2017. Decoupling of Mg-C and Sr-Nd-O Isotopes Traces the Role of Recycled Carbon in Magnesiocarbonatites from the Tarim Large Igneous Province. *Geochimica et Cosmochimica Acta*, 202: 159–178. <https://doi.org/10.1016/j.gca.2016.12.036>
- CIAAW, 2019. Atomic Weights of the Elements 2019. <https://ciaaw.org/atomic-weights.htm>
- Dai, L. Q., Zhao, K., Zhao, Z. F., et al., 2020. Magnesium-Carbon Isotopes Trace Carbon Recycling in Continental Subduction Zone. *Lithos*, 376–377: 105774. <https://doi.org/10.1016/j.lithos.2020.105774>
- Dai, M. N., Bao, Z. A., Chen, K. Y., et al., 2016. In-Situ Analysis of Mg Isotopic Compositions of Basalt Glasses by Femtosecond Laser Ablation Multi-Collector Inductively Coupled Mass Spectrometry. *Chinese Journal of Analytical Chemistry*, 44(2): 173–178 (in Chinese with English abstract).
- Dessert, C., Lajeunesse, E., Lloret, E., et al., 2015. Controls on Chemical Weathering on a Mountainous Volcanic Tropical Island: Guadeloupe (French West Indies). *Geochimica et Cosmochimica Acta*, 171: 216–237. <https://doi.org/10.1016/j.gca.2015.09.009>
- Dong, A. G., Han, G. L., 2017. A Review of Magnesium Isotope System in Rivers. *Advances in Earth Science*, 32(8): 800–809 (in Chinese with English abstract).
- Dong, A. G., Zhu, X. K., 2016. Mg Isotope Geochemical Cycle in Supergene Environment. *Advances in Earth Science*, 31(1): 43–58 (in Chinese with English abstract).
- D' Orazio, M., Armienti, P., Cerretini, S., 1998. Phenocryst/Matrix Trace - Element Partition Coefficients for Hawaiite-Trachyte Lavas from the Ellittico Volcanic Sequence (Mt. Etna, Sicily, Italy). *Mineralogy and Petrology*, 64(1–4): 65–88. <https://doi.org/10.1007/BF01226564>
- Doroshkevich, A. G., Veksler, I. V., Klemd, R., et al., 2017. Trace - Element Composition of Minerals and Rocks in the Belaya Zima Carbonatite Complex (Russia): Implications for the Mechanisms of Magma Evolution and Carbonatite Formation. *Lithos*, 284–285: 91–108. <https://doi.org/10.1016/j.lithos.2017.04.003>
- Fan, B. L., Tao, F. X., Zhao, Z. Q., 2013. Advance of Geochemical Applications of Magnesium Isotope in Marine and Earth Surface Environments. *Bulletin of Mineralogy, Petrology and Geochemistry*, 32(1): 114–120 (in Chinese with English abstract).
- Fan, H. R., Niu, H. C., Li, X. C., et al., 2020. The Types, Ore Genesis and Resource Perspective of Endogenic REE Deposits in China. *Chinese Science Bulletin*, 65(33): 3778–3793 (in Chinese).
- Fries, D. M., James, R. H., Dessert, C., et al., 2019. The Response of Li and Mg Isotopes to Rain Events in a Highly-Weathered Catchment. *Chemical Geology*, 519: 68–82. <https://doi.org/10.1016/j.chemgeo.2019.04.023>
- Galy, A., Yoffe, O., Janney, P. E., et al., 2003. Magnesium Isotope Heterogeneity of the Isotopic Standard SRM980 and New Reference Materials for Magnesium - Isotope - Ratio Measurements. *Journal of Analytical Atomic Spectrometry*, 18(11): 1352–1356. <https://doi.org/10.1039/b309273a>
- Galy, A., Belshaw, N. S., Halicz, L., et al., 2001. High-Precision Measurement of Magnesium Isotopes by Multiple-Collector Inductively Coupled Plasma Mass Spectrometry. *International Journal of Mass Spectrometry*, 208(1–3): 89–98. [https://doi.org/10.1016/s1387-3806\(01\)00380-3](https://doi.org/10.1016/s1387-3806(01)00380-3)
- Gao, T., Ke, S., Li, R. Y., et al., 2019. High-Precision Magnesium Isotope Analysis of Geological and Environmental Reference Materials by Multiple - Collector Inductively Coupled Plasma Mass Spectrometry. *Rapid Communications in Mass Spectrometry*, 33(8): 767–777. <https://doi.org/10.1002/rcm.8376>
- Gao, T., Ke, S., Wang, S. J., et al., 2018. Contrasting Mg Isotopic Compositions between Fe - Mn Nodules and Surrounding Soils: Accumulation of Light Mg Isotopes by Mg-Depleted Clay Minerals and Fe Oxides. *Geochimica et Cosmochimica Acta*, 237: 205–222. <https://doi.org/>

- 10.1016/j.gca.2018.06.028
- Geske, A., Goldstein, R.H., Mavromatis, V., et al., 2015. The Magnesium Isotope ( $\delta^{26}\text{Mg}$ ) Signature of Dolomites. *Geochimica et Cosmochimica Acta*, 149: 131–151. <https://doi.org/10.1016/j.gca.2014.11.003>
- Gray, C.M., Compston, W., 1974. Excess  $^{26}\text{Mg}$  in the Allende Meteorite. *Nature*, 251: 495–497. <https://doi.org/10.1038/251495a0>
- Guo, B.J., Zhu, X.K., Dong A.G., et al., 2019. Mg Isotopic Systematics and Geochemical Applications: A Critical Review. *Journal of Asian Earth Sciences*, 176: 368–385. <https://doi.org/10.1016/j.jseae.2019.03.001>
- Halama, R., McDonough, W.F., Rudnick, R.L., et al., 2007. The Li Isotopic Composition of Oldoinyo Lengai: Nature of the Mantle Sources and Lack of Isotopic Fractionation during Carbonatite Petrogenesis. *Earth and Planetary Science Letters*, 254(1–2): 77–89. <https://doi.org/10.1016/j.epsl.2006.11.022>
- Halama, R., McDonough, W.F., Rudnick, R.L., et al., 2008. Tracking the Lithium Isotopic Evolution of the Mantle Using Carbonatites. *Earth and Planetary Science Letters*, 265(3–4): 726–742. <https://doi.org/10.1016/j.epsl.2007.11.007>
- Hammouda, T., Keshav, S., 2015. Melting in the Mantle in the Presence of Carbon: Review of Experiments and Discussion on the Origin of Carbonatites. *Chemical Geology*, 418: 171–188. <https://doi.org/10.1016/j.chemgeo.2015.05.018>
- Handler, M.R., Baker, J.A., Schiller, M., et al., 2009. Magnesium Stable Isotope Composition of Earth's Upper Mantle. *Earth and Planetary Science Letters*, 282(1–4): 306–313. <https://doi.org/10.1016/j.epsl.2009.03.031>
- Harrison, A.L., Bénézech, P., Schott, J., et al., 2021. Magnesium and Carbon Isotope Fractionation during Hydrated Mg-Carbonate Mineral Phase Transformations. *Geochimica et Cosmochimica Acta*, 293: 507–524. <https://doi.org/10.1016/j.gca.2020.10.028>
- He, R., Ning, M., Huang, K.J., et al., 2020. Mg Isotopic Systematics during Early Diagenetic Aragonite-Calcite Transition: Insights from the Key Largo Limestone. *Chemical Geology*, 558: 119876. <https://doi.org/10.1016/j.chemgeo.2020.119876>
- He, X.X., Zhu, X.K., Li, S.Z., et al., 2008. High-Precision Measurement of Magnesium Isotopes Using MC-ICP-MS. *Acta Petrologica et Mineralogica*, 27(5): 441–448 (in Chinese with English abstract).
- Heymann, D., Dziczkaniec, M., 1976. Early Irradiation of Matter in the Solar System: Magnesium (Proton, Neutron) Scheme. *Science*, 191(4222): 79–81. <https://doi.org/10.1126/science.191.4222.79>
- Hindshaw, R.S., Teisserenc, R., Le Dantec, T., et al., 2019. Seasonal Change of Geochemical Sources and Processes in the Yenisei River: A Sr, Mg and Li Isotope Study. *Geochimica et Cosmochimica Acta*, 255: 222–236. <https://doi.org/10.1016/j.gca.2019.04.015>
- Hindshaw, R.S., Tosca, R., Tosca, N.J., et al., 2020. Experimental Constraints on Mg Isotope Fractionation during Clay Formation: Implications for the Global Biogeochemical Cycle of Mg. *Earth and Planetary Science Letters*, 531: 115980. <https://doi.org/10.1016/j.epsl.2019.115980>
- Hoang, T.H.A., Choi, S.H., Yu, Y., et al., 2018. Geochemical Constraints on the Spatial Distribution of Recycled Oceanic Crust in the Mantle Source of Late Cenozoic Basalts, Vietnam. *Lithos*, 296–299: 382–395. <https://doi.org/10.1016/j.lithos.2017.11.020>
- Hou, Z.Q., Chen, J., Zhai, M.G., 2020. Current Status and Frontiers of Research on Critical Mineral Resources. *Chinese Science Bulletin*, 65(33): 3651–3652 (in Chinese).
- Hou, Z.Q., Liu, Y., Tian, S.H., et al., 2015. Formation of Carbonatite-Related Giant Rare-Earth-Element Deposits by the Recycling of Marine Sediments. *Scientific Reports*, 5(1): 10231. <https://doi.org/10.1038/srep10231>
- Hu, Y., Teng, F.Z., Plank, T., et al., 2017b. Magnesium Isotopic Composition of Subducting Marine Sediments. *Chemical Geology*, 466: 15–31. <https://doi.org/10.1016/j.chemgeo.2017.06.010>
- Hu, Y., Teng, F.Z., Zhang, H.F., et al., 2016. Metasomatism-Induced Mantle Magnesium Isotopic Heterogeneity: Evidence from Pyroxenites. *Geochimica et Cosmochimica Acta*, 185: 88–111. <https://doi.org/10.1016/j.gca.2015.11.001>
- Hu, Z.Y., Hu, W.X., Liu, C., et al., 2019. Conservative Behavior of Mg Isotopes in Massive Dolostones: From Diagenesis to Hydrothermal Reworking. *Sedimentary Geology*, 381: 65–75. <https://doi.org/10.1016/j.sedgeo.2018.12.007>
- Hu, Z.Y., Hu, W.X., Wang, X.M., et al., 2017a. Resetting of Mg Isotopes between Calcite and Dolomite during Burial Metamorphism: Outlook of Mg Isotopes as Geothermometer and Seawater Proxy. *Geochimica et Cosmochimica Acta*, 208: 24–40. <https://doi.org/10.1016/j.gca.2017.03.026>
- Huang, F., Chakraborty, P., Lundstrom, C.C., et al., 2010. Isotope Fractionation in Silicate Melts by Thermal Diffusion. *Nature*, 464: 396–400. <https://doi.org/10.1038/nature10764>
- Huang, F., Glessner, J., Ianno, A., et al., 2009. Magnesium Isotopic Composition of Igneous Rock Standards Measured



- by MC-ICP-MS. *Chemical Geology*, 268(1–2):15–23. <https://doi.org/10.1016/j.chemgeo.2009.07.003>
- Huang, F., Zhang, Z. F., Lundstrom, C. C., et al., 2011. Iron and Magnesium Isotopic Compositions of Peridotite Xenoliths from Eastern China. *Geochimica et Cosmochimica Acta*, 75(12): 3318–3334. <https://doi.org/10.1016/j.gca.2011.03.036>
- Huang, J., Huang, F., Xiao, Y. L., 2019. Fe-Mg Isotopic Compositions of Altered Oceanic Crust and Subduction-Zone Fluids. *Earth Science*, 44(12): 4050–4056(in Chinese with English abstract). <https://doi.org/10.3799/dqkx.2019.234>
- Huang, J., Ke, S., Gao, Y. J., et al., 2015b. Magnesium Isotopic Compositions of Altered Oceanic Basalts and Gabbros from IODP Site 1256 at the East Pacific Rise. *Lithos*, 231: 53–61. <https://doi.org/10.1016/j.lithos.2015.06.009>
- Huang, J., Li, S. G., Xiao Y. L., et al., 2015a. Origin of Low  $\delta^{26}\text{Mg}$  Cenozoic Basalts from South China Block and Their Geodynamic Implications. *Geochimica et Cosmochimica Acta*, 164:298–317. <https://doi.org/10.1016/j.gca.2015.04.054>
- Huang, J., Xiao, Y. L., 2016. Mg-Sr Isotopes of Low- $\delta^{26}\text{Mg}$  Basalts Tracing Recycled Carbonate Species: Implication for the Initial Melting Depth of the Carbonated Mantle in Eastern China. *International Geology Review*, 58(11): 1350–1362. <https://doi.org/10.1080/00206814.2016.1157709>
- Huang, K. J., Shen, B., Lang, X. G., et al., 2015c. Magnesium Isotopic Compositions of the Mesoproterozoic Dolostones: Implications for Mg Isotopic Systematics of Marine Carbonates. *Geochimica et Cosmochimica Acta*, 164: 333–351. <https://doi.org/10.1016/j.gca.2015.05.002>
- Huang, K. J., Teng, F. Z., Elsenouy, A., et al., 2013. Magnesium Isotopic Variations in Loess: Origins and Implications. *Earth and Planetary Science Letters*, 374: 60–70. <https://doi.org/10.1016/j.epsl.2013.05.010>
- Huang, K. J., Teng, F. Z., Plank, T., et al., 2018. Magnesium Isotopic Composition of Altered Oceanic Crust and the Global Mg Cycle. *Geochimica et Cosmochimica Acta*, 238: 357–373. <https://doi.org/10.1016/j.gca.2018.07.011>
- Jiang, S. Y., Wen, H. J., Xu, C., et al., 2019. Earth Sphere Cycling and Enrichment Mechanism of Critical Metals: Major Scientific Issues for Future Research. *Bulletin of National Natural Science Foundation of China*, 33(2): 112–118(in Chinese with English abstract).
- Jin, M., Feng, D., Huang, K. J., et al., 2021. Behavior of Mg Isotopes during Precipitation of Methane-Derived Carbonate: Evidence from Tubular Seep Carbonates from the South China Sea. *Chemical Geology*, 567: 120101. <https://doi.org/10.1016/j.chemgeo.2021.120101>
- Jung, S. G., Choi, S. H., Ji, K. H., et al., 2019. Geochemistry of Volcanic Rocks from Oldoinyo Lengai, Tanzania: Implications for Mantle Source Lithology. *Lithos*, 350–351: 105223. <https://doi.org/10.1016/j.lithos.2019.105223>
- Ke, S., Liu, S. A., Li, W. Y., et al., 2011. Advances and Application in Magnesium Isotope Geochemistry. *Acta Petrologica Sinica*, 27(2): 383–397(in Chinese with English abstract).
- Ke, S., Teng, F. Z., Li, S. G., et al., 2016. Mg, Sr, and O Isotope Geochemistry of Syenites from Northwest Xinjiang, China: Tracing Carbonate Recycling during Tethyan Oceanic Subduction. *Chemical Geology*, 437: 109–119. <https://doi.org/10.1016/j.chemgeo.2016.05.002>
- Kim, J. I., Choi, S. H., Koh, G. W., et al., 2019. Petrogenesis and Mantle Source Characteristics of Volcanic Rocks on Jeju Island, South Korea. *Lithos*, 326–327: 476–490. <https://doi.org/10.1016/j.lithos.2018.12.034>
- Ku, Y., Jacobsen, S. B., 2020. Potassium Isotope Anomalies in Meteorites Inherited from the Protosolar Molecular Cloud. *Science Advances*, 6(41): eabd0511. <https://doi.org/10.1126/sciadv.abd0511>
- Lai, Y. J., Pogge von Strandmann, P. A. E., Dohmen, R., et al., 2015. The Influence of Melt Infiltration on the Li and Mg Isotopic Composition of the Horoman Peridotite Massif. *Geochimica et Cosmochimica Acta*, 164: 318–332. <https://doi.org/10.1016/j.gca.2015.05.006>
- Lee, S. G., Ahn, I., Asahara, Y., et al., 2018. Geochemical Interpretation of Magnesium and Oxygen Isotope Systematics in Granites with the REE Tetrad Effect. *Geosciences Journal*, 22(5): 697–710. <https://doi.org/10.1007/s12303-018-0024-1>
- Lee, S. W., Ryu, J. S., Lee, K. S., 2014. Magnesium Isotope Geochemistry in the Han River, South Korea. *Chemical Geology*, 364: 9–19. <https://doi.org/10.1016/j.chemgeo.2013.11.022>
- Lee, T., Papanastassiou, D. A., 1974. Mg Isotopic Anomalies in the Allende Meteorite and Correlation with O and Sr Effects. *Geophysical Research Letters*, 1(6): 225–228. <https://doi.org/10.1029/GL001i006p00225>
- Li, L. B., Zhang, F., Jin, Z. D., et al., 2020. Riverine Mg Isotopes Response to Glacial Weathering within the Muztag Catchment of the Eastern Pamir Plateau. *Applied Geochemistry*, 118:104626. <https://doi.org/10.1016/j.apgeochem.2020.104626>
- Li, M. Y. H., Teng, F. Z., Zhou, M. F., 2021a. Phyllosilicate

- Controls on Magnesium Isotopic Fractionation during Weathering of Granites: Implications for Continental Weathering and Riverine System. *Earth and Planetary Science Letters*, 553: 116613. <https://doi.org/10.1016/j.epsl.2020.116613>
- Li, M.L., Liu, S.G., Lee, H.Y., et al., 2021b. Magnesium and Zinc Isotopic Anomaly of Cenozoic Lavas in Central Myanmar: Origins and Implications for Deep Carbon Recycling. *Lithos*, 386–387: 106011. <https://doi.org/10.1016/j.lithos.2021.106011>
- Li, R.Y., Ke, S., He, Y.S., et al., 2016. High Precision Magnesium Isotope Measurement for High-Cr Samples. *Bulletin of Mineralogy, Petrology and Geochemistry*, 35(3): 441–447 (in Chinese with English abstract).
- Li, S.G., 2015. Tracing Deep Carbon Recycling by Mg Isotopes. *Earth Science Frontiers*, 2015, 22(5): 143–159 (in Chinese with English abstract).
- Li, S.G., Yang, W., Ke, S., et al., 2017. Deep Carbon Cycles Constrained by a Large-Scale Mantle Mg Isotope Anomaly in Eastern China. *National Science Review*, 4(1): 111–120. <https://doi.org/10.1093/nsr/nww070>
- Li, S.Z., Zhu, X.K., He, X.X., et al., 2008. Separation of Mg for Isotope Determination by MC-ICP-MS. *Acta Petrologica et Mineralogica*, 27(5): 449–456 (in Chinese with English abstract).
- Li, W.Q., Zhao, S.G., Wang, X.M., et al., 2020. Fingerprinting Hydrothermal Fluids in Porphyry Cu Deposits Using K and Mg Isotopes. *Science China: Earth Sciences*, 50(2): 245–257 (in Chinese).
- Li, W.Y., Teng, F.Z., Halama, R., et al., 2016. Magnesium Isotope Fractionation during Carbonatite Magmatism at Oldoinyo Lengai, Tanzania. *Earth and Planetary Science Letters*, 444: 26–33. <https://doi.org/10.1016/j.epsl.2016.03.034>
- Li, W.Y., Teng, F.Z., Ke, S., et al., 2010. Heterogeneous Magnesium Isotopic Composition of the Upper Continental Crust. *Geochimica et Cosmochimica Acta*, 74(23): 6867–6884. <https://doi.org/10.1016/j.gca.2010.08.030>
- Li, W.Y., Teng, F.Z., Wing, B.A., et al., 2014. Limited Magnesium Isotope Fractionation during Metamorphic Dehydration in Metapelites from the Onawa Contact Aureole, Maine. *Geochemistry, Geophysics, Geosystems*, 15(2): 408–415. <https://doi.org/10.1002/2013gc004992>
- Li, W.Y., Teng, F.Z., Xiao, Y.L., et al., 2011. High-Temperature Inter-Mineral Magnesium Isotope Fractionation in Eclogite from the Dabie Orogen, China. *Earth and Planetary Science Letters*, 304(1–2): 224–230. <https://doi.org/10.1016/j.epsl.2011.01.035>
- Ling, M.X., Liu, Y.L., Williams, I.S., et al., 2013. Formation of the World's Largest REE Deposit through Protracted Fluxing of Carbonatite by Subduction-Derived Fluids. *Scientific Reports*, 3: 1776. <https://doi.org/10.1038/srep01776>
- Litasov, K.D., Goncharov, A.F., Hemley, R.J., 2011. Cross-over from Melting to Dissociation of CO<sub>2</sub> under Pressure: Implications for the Lower Mantle. *Earth and Planetary Science Letters*, 309(3–4): 318–323. <https://doi.org/10.1016/j.epsl.2011.07.006>
- Liu, D., Zhao, Z.D., Zhu, D.C., et al., 2015. Identifying Mantle Carbonatite Metasomatism through Os-Sr-Mg Isotopes in Tibetan Ultrapotassic Rocks. *Earth and Planetary Science Letters*, 430: 458–469. <https://doi.org/10.1016/j.epsl.2015.09.005>
- Liu, F., Li, X., Wang, G.Q., et al., 2017b. Marine Carbonate Component in the Mantle beneath the Southeastern Tibetan Plateau: Evidence from Magnesium and Calcium Isotopes. *Journal of Geophysical Research: Solid Earth*, 122(12): 9729–9744. <https://doi.org/10.1002/2017jb014206>
- Liu, P.P., Teng, F.Z., Dick, H.J.B., et al., 2017a. Magnesium Isotopic Composition of the Oceanic Mantle and Oceanic Mg Cycling. *Geochimica et Cosmochimica Acta*, 206: 151–165. <https://doi.org/10.1016/j.gca.2017.02.016>
- Liu, S.A., Li, S.G., 2019. Tracing the Deep Carbon Cycle Using Metal Stable Isotopes: Opportunities and Challenges. *Engineering*, 5(3): 448–457. <https://doi.org/10.1016/j.eng.2019.03.007>
- Liu, S.A., Teng, F.Z., He, Y.S., et al., 2010. Investigation of Magnesium Isotope Fractionation during Granite Differentiation: Implication for Mg Isotopic Composition of the Continental Crust. *Earth and Planetary Science Letters*, 297(3–4): 646–654. <https://doi.org/10.1016/j.epsl.2010.07.019>
- Liu, S.A., Teng, F.Z., Yang, W., et al., 2011. High-Temperature Inter-Mineral Magnesium Isotope Fractionation in Mantle Xenoliths from the North China Craton. *Earth and Planetary Science Letters*, 308(1–2): 131–140. <https://doi.org/10.1016/j.epsl.2011.05.047>
- Liu, X.M., Teng, F.Z., Rudnick, R.L., et al., 2014. Massive Magnesium Depletion and Isotope Fractionation in Weathered Basalts. *Geochimica et Cosmochimica Acta*, 135: 336–349. <https://doi.org/10.1016/j.gca.2014.03.028>
- Liu, Y., Chen, C., Shu, X.C., et al., 2017. The Formation Model of the Carbonatite-Syenite Complex REE Deposits in the East of Tibetan Plateau: A Case Study of Dalucao REE Deposit. *Acta Petrologica Sinica*, 33(7): 1978–2000. (in Chinese with English abstract).

- Luo, H. Y., Karki, B. B., Ghosh, D. B., et al., 2020. First-Principles Computation of Diffusional Mg Isotope Fractionation in Silicate Melts. *Geochimica et Cosmochimica Acta*, 290: 27–40. <https://doi.org/10.1016/j.gca.2020.08.028>
- Macris, C. A., Young, E. D., Manning, C. E., 2013. Experimental Determination of Equilibrium Magnesium Isotope Fractionation between Spinel, Forsterite, and Magnesite from 600 to 800 °C. *Geochimica et Cosmochimica Acta*, 118:18–32. <https://doi.org/10.1016/j.gca.2013.05.008>
- Mao, J. W., Yuan, S. D., Xie, G. Q., et al., 2019. New Advances on Metallogenic Studies and Exploration on Critical Minerals of China in 21st Century. *Mineral Deposits*, 38(5):935–969(in Chinese with English abstract).
- Moynier, F., Hu, Y., Dai, W., et al., 2021b. Potassium Isotopic Composition of Seven Widely Available Biological Standards Using Collision Cell (CC)-MC-ICP-MS. *Journal of Analytical Atomic Spectrometry*. <https://doi.org/10.1039/d1ja00294e>
- Moynier, F., Hu, Y., Wang, K., et al., 2021a. Potassium Isotopic Composition of Various Samples Using a Dual-Path Collision Cell-Capable Multiple-Collector Inductively Coupled Plasma Mass Spectrometer, Nu Instruments Sapphire. *Chemical Geology*, 571: 120144. <https://doi.org/10.1016/j.chemgeo.2021.120144>
- Nitzsche, K. N., Kato, Y., Shin, K. C., et al., 2019. Magnesium Isotopes Reveal Bedrock Impacts on Stream Organisms. *Science of the Total Environment*, 688:243–252. <https://doi.org/10.1016/j.scitotenv.2019.06.209>
- Oeser, M., Dohmen, R., Horn, I., et al., 2015. Processes and Time Scales of Magmatic Evolution as Revealed by Fe-Mg Chemical and Isotopic Zoning in Natural Olivines. *Geochimica et Cosmochimica Acta*, 154:130–150. <https://doi.org/10.1016/j.gca.2015.01.025>
- Oeser, M., Weyer, S., Horn, I., et al., 2014. High-Precision Fe and Mg Isotope Ratios of Silicate Reference Glasses Determined In Situ by Femtosecond LA-MC-ICP-MS and by Solution Nebulisation MC-ICP-MS. *Geostandards and Geoanalytical Research*, 38(3): 311–328. <https://doi.org/10.1111/j.1751-908X.2014.00288.x>
- Oi, T., Yanase, S., Kakihana, H., 1987. Magnesium Isotope Fractionation in Cation-Exchange Chromatography. *Separation Science and Technology*, 22(11): 2203–2215. <https://doi.org/10.1080/01496398708068608>
- Oskierski, H. C., Beinlich, A., Mavromatis, V., et al., 2019. Mg Isotope Fractionation during Continental Weathering and Low Temperature Carbonation of Ultramafic Rocks. *Geochimica et Cosmochimica Acta*, 262:60–77. <https://doi.org/10.1016/j.gca.2019.07.019>
- Pang, K. N., Teng, F. Z., Sun, Y., et al., 2020. Magnesium Isotopic Systematics of the Makran Arc Magmas, Iran: Implications for Crust-Mantle Mg Isotopic Balance. *Geochimica et Cosmochimica Acta*, 278:110–121. <https://doi.org/10.1016/j.gca.2019.10.005>
- Pogge von Strandmann, P. A. E., Dohmen, R., Marschall, H. R., et al., 2015. Extreme Magnesium Isotope Fractionation at Outcrop Scale Records the Mechanism and Rate at which Reaction Fronts Advance. *Journal of Petrology*, 56(1):33–58. <https://doi.org/10.1093/petrology/egu07>
- Pogge von Strandmann, P. A. E., Elliott, T., Marschall, H. R., et al., 2011. Variations of Li and Mg Isotope Ratios in Bulk Chondrites and Mantle Xenoliths. *Geochimica et Cosmochimica Acta*, 75(18): 5247–5268. <https://doi.org/10.1016/j.gca.2011.06.026>
- Pogge von Strandmann, P. A. E., Hendry, K. R., Hatton, J. E., et al., 2019. The Response of Magnesium, Silicon, and Calcium Isotopes to Rapidly Uplifting and Weathering Terrains: South Island, New Zealand. *Frontiers in Earth Science*, 7: 240. <https://doi.org/10.3389/feart.2019.00240>
- Richter, F. M., Watson, E. B., Mendybaev, R. A., et al., 2008. Magnesium Isotope Fractionation in Silicate Melts by Chemical and Thermal Diffusion. *Geochimica et Cosmochimica Acta*, 72(1):206–220. <https://doi.org/10.1016/j.gca.2007.10.016>
- Ringwood, A. E., 1990. Slab-Mantle Interactions: 3. Petrogenesis of Intraplate Magmas and Structure of the Upper Mantle. *Chemical Geology*, 82: 187–207. [https://doi.org/10.1016/0009-2541\(90\)90081-H](https://doi.org/10.1016/0009-2541(90)90081-H)
- Ryu, J. S., Vigier, N., Derry, L., et al., 2021. Variations of Mg Isotope Geochemistry in Soils over a Hawaiian 4 Myr Chronosequence. *Geochimica et Cosmochimica Acta*, 292:94–114. <https://doi.org/10.1016/j.gca.2020.09.024>
- Saenger, C., Wang, Z. R., 2014. Magnesium Isotope Fractionation in Biogenic and Abiogenic Carbonates: Implications for Paleoenvironmental Proxies. *Quaternary Science Reviews*, 90: 1–21. <https://doi.org/10.1016/j.quascirev.2014.01.014>
- Schauble, E. A., 2011. First-Principles Estimates of Equilibrium Magnesium Isotope Fractionation in Silicate, Oxide, Carbonate and Hexaaquamagnesium(2+) Crystals. *Geochimica et Cosmochimica Acta*, 75(3):844–869. <https://doi.org/10.1016/j.gca.2010.09.044>
- Sedaghatpour, F., Teng, F. Z., 2016. Magnesium Isotopic Composition of Achondrites. *Geochimica et Cosmochimica Acta*, 174: 167–179. <https://doi.org/10.1016/j.gca.2015.11.016>
- Seto, Y., Hamane, D., Nagai, T., et al., 2008. Fate of Carbon-

- ates within Oceanic Plates Subducted to the Lower Mantle, and a Possible Mechanism of Diamond Formation. *Physics and Chemistry of Minerals*, 35(4): 223–229. <https://doi.org/10.1007/s00269-008-0215-9>
- Shalev, N., Bontognali, T.R.R., Vance, D., 2021. Sabkha Dolomite as an Archive for the Magnesium Isotope Composition of Seawater. *Geology*, 49(3): 253–257. <https://doi.org/10.1130/g47973.1>
- Shen, J., Li, W.Y., Li, S.G., et al., 2019. Crust-Mantle Interactions at Different Depths in the Subduction Channel: Magnesium Isotope Records of Ultramafic Rocks from the Mantle Wedges. *Earth Science*, 44(12): 4102–4111 (in Chinese with English abstract).
- Sio, C.K.I., Dauphas, N., Teng, F.Z., et al., 2013. Discerning Crystal Growth from Diffusion Profiles in Zoned Olivine by In Situ Mg-Fe Isotopic Analyses. *Geochimica et Cosmochimica Acta*, 123: 302–321. <https://doi.org/10.1016/j.gca.2013.06.008>
- Solopova, N.A., Dubrovinsky, L., Spivak, A.V., et al., 2015. Melting and Decomposition of MgCO<sub>3</sub> at Pressures up to 84 GPa. *Physics and Chemistry of Minerals*, 42(1): 73–81. <https://doi.org/10.1007/s00269-014-0701-1>
- Song, W.L., Xu, C., Chakhmouradian, A.R., et al., 2017. Carbonatites of Tarim (NW China): First Evidence of Crustal Contribution in Carbonatites from a Large Igneous Province. *Lithos*, 282–283: 1–9. <https://doi.org/10.1016/j.lithos.2017.02.018>
- Song, W.L., Xu, C., Smith, M.P., et al., 2016. Origin of Unusual HREE-Mo-Rich Carbonatites in the Qinling Orogen, China. *Scientific Reports*, 6: 37377. <https://doi.org/10.1038/srep37377>
- Song, W.L., Xu, C., Wang, L.J., et al., 2013. Review of the Metallogensis of the Endogenetic Rare Earth Elements Deposits Related to Carbonatite-Alkaline Complex. *Acta Scientiarum Naturalium Universitatis Pekinensis*, 49(4): 725–740 (in Chinese with English abstract).
- Su, B.X., Hu, Y., Teng, F.Z., et al., 2017a. Chromite-Induced Magnesium Isotope Fractionation during Mafic Magma Differentiation. *Science Bulletin*, 62(22): 1538–1546. <https://doi.org/10.1016/j.scib.2017.11.001>
- Su, B.X., Hu, Y., Teng, F.Z., et al., 2017b. Magnesium Isotope Constraints on Subduction Contribution to Mesozoic and Cenozoic East Asian Continental Basalts. *Chemical Geology*, 466: 116–122. <https://doi.org/10.1016/j.chemgeo.2017.05.026>
- Su, B.X., Hu, Y., Teng, F.Z., et al., 2019a. Light Mg Isotopes in Mantle-Derived Lavas Caused by Chromite Crystallization, Instead of Carbonatite Metasomatism. *Earth and Planetary Science Letters*, 522: 79–86. <https://doi.org/10.1016/j.epsl.2019.06.016>
- Su, B.X., Xiao, Y., Chen, C., et al., 2018. Potential Applications of Fe and Mg Isotopes in Genesis of Chromite Deposits in Ophiolites. *Earth Science*, 43(4): 1011–1024 (in Chinese with English abstract). <https://doi.org/10.3799/dqkx.2018.705>
- Su, J.H., Zhao, X.F., Li, X.C., et al., 2019b. Geological and Geochemical Characteristics of the Miaoya Syenite-Carbonatite Complex, Central China: Implications for the Origin of REE-Nb-Enriched Carbonatite. *Ore Geology Reviews*, 113: 103101. <https://doi.org/10.1016/j.oregeorev.2019.103101>
- Sun, J., Zhu, X.K., Belshaw, N.S., et al., 2021c. Ca Isotope Systematics of Carbonatites: Insights into Carbonatite Source and Evolution. *Geochemical Perspectives Letters*, 11–15. <https://doi.org/10.7185/geochemlet.2107>
- Sun, J., Zhu, X.K., Chen, Y.L., et al., 2012. Fe Isotope Compositions of Related Geological Formation in Bayan Obo Area and Their Constrains on the Genesis of Bayan Obo Ore Deposit. *Acta Geologica Sinica*, 86(5): 819–828 (in Chinese with English abstract).
- Sun, Y., Teng, F.Z., Pang, K.N., 2021b. The Presence of Paleo-Pacific Slab beneath Northwest North China Craton Hinted by Low- $\delta^{26}\text{Mg}$  Basalts at Wulanhada. *Lithos*, 386–387: 106009. <https://doi.org/10.1016/j.lithos.2021.106009>
- Sun, Y., Teng, F.Z., Pang, K.N., et al., 2021a. Multistage Mantle Metasomatism Deciphered by Mg-Sr-Nd-Pb Isotopes in the Leucite Hills Lamproïtes. *Contributions to Mineralogy and Petrology*, 176(6): 1–12. <https://doi.org/10.1007/s00410-021-01801-9>
- Sun, Y., Teng, F.Z., Ying, J.F., et al., 2017. Magnesium Isotopic Evidence for Ancient Subducted Oceanic Crust in LOMU-Like Potassium-Rich Volcanic Rocks. *Journal of Geophysical Research: Solid Earth*, 122(10): 7562–7572. <https://doi.org/10.1002/2017JB014560>
- Tang, Q.Y., Bao, J., Dang, Y.X., et al., 2018. Mg-Sr-Nd Isotopic Constraints on the Genesis of the Giant Jinchuan Ni-Cu-(PGE) Sulfide Deposit, NW China. *Earth and Planetary Science Letters*, 502: 221–230. <https://doi.org/10.1016/j.epsl.2018.09.008>
- Taylor, W.R., Green, D.H., 1988. Measurement of Reduced Peridotite-C-O-H Solidus and Implications for Redox Melting of the Mantle. *Nature*, 332(6162): 349–352. <https://doi.org/10.1038/332349a0>
- Teng, F.Z., 2017. Magnesium Isotope Geochemistry. *Reviews in Mineralogy and Geochemistry*, 82(1): 219–287. <https://doi.org/10.2138/rmg.2017.82.7>
- Teng, F.Z., Dauphas, N., Helz, R.T., et al., 2011. Diffusion-

- Driven Magnesium and Iron Isotope Fractionation in Hawaiian Olivine. *Earth and Planetary Science Letters*, 308 (3–4): 317–324. <https://doi.org/10.1016/j.epsl.2011.06.003>
- Teng, F.Z., Dauphas, N., Watkins, J.M., 2017. Non-Traditional Stable Isotopes: Retrospective and Prospective. *Reviews in Mineralogy and Geochemistry*, 82(1): 1–26. <https://doi.org/10.2138/rmg.2017.82.1>
- Teng, F.Z., Hu, Y., Chauvel, C., 2016. Magnesium Isotope Geochemistry in Arc Volcanism. *Proceedings of the National Academy of Sciences of the United States of America*, 113(26):7082–7087. <https://doi.org/10.1073/pnas.1518456113>
- Teng, F.Z., Li, W.Y., Ke, S., et al., 2010a. Magnesium Isotopic Composition of the Earth and Chondrites. *Geochimica et Cosmochimica Acta*, 74(14): 4150–4166. <https://doi.org/10.1016/j.gca.2010.04.019>
- Teng, F.Z., Li, W.Y., Rudnick, R.L., et al., 2010b. Contrasting Lithium and Magnesium Isotope Fractionation during Continental Weathering. *Earth and Planetary Science Letters*, 300(1/2):63–71. <https://doi.org/10.1016/j.epsl.2010.09.036>
- Teng, F.Z., Li, W.Y., Ke, S., et al., 2015. Magnesium Isotopic Compositions of International Geological Reference Materials. *Geostandards and Geoanalytical Research*, 39(3): 329–339. <https://doi.org/10.1111/j.1751-908X.2014.00326.x>
- Teng, F.Z., Wadhwa, M., Helz, R.T., 2007. Investigation of Magnesium Isotope Fractionation during Basalt Differentiation: Implications for a Chondritic Composition of the Terrestrial Mantle. *Earth and Planetary Science Letters*, 261(1): 84–92. <https://doi.org/10.1016/j.epsl.2007.06.004>
- Teng, F.Z., Yang, W., 2014. Comparison of Factors Affecting the Accuracy of High-Precision Magnesium Isotope Analysis by Multi-Collector Inductively Coupled Plasma Mass Spectrometry. *Rapid Communications in Mass Spectrometry*, 28(1): 19–24. <https://doi.org/10.1002/rcm.6752>
- Teng, F.Z., Yang, W., Rudnick, R.L., et al., 2013. Heterogeneous Magnesium Isotopic Composition of the Lower Continental Crust: A Xenolith Perspective. *Geochemistry, Geophysics, Geosystems*, 14(9): 3844–3856. <https://doi.org/10.1002/ggge.20238>
- Tian, H.C., Teng, F.Z., Hou, Z.Q., et al., 2020b. Magnesium and Lithium Isotopic Evidence for a Remnant Oceanic Slab beneath Central Tibet. *Journal of Geophysical Research: Solid Earth*, 125(1): e2019JB018197. <https://doi.org/10.1029/2019JB018197>
- Tian, H.C., Yang, W., Li, S.G., et al., 2016. Origin of Low  $\delta^{26}\text{Mg}$  Basalts with EM-I Component: Evidence for Interaction between Enriched Lithosphere and Carbonated Asthenosphere. *Geochimica et Cosmochimica Acta*, 188: 93–105. <https://doi.org/10.1016/j.gca.2016.05.021>
- Tian, H.C., Yang, W., Li, S.G., et al., 2019. Approach to Trace Hidden Paleo-Weathering of Basaltic Crust through Decoupled Mg, Sr and Nd Isotopes Recorded in Volcanic Rocks. *Chemical Geology*, 509: 234–248. <https://doi.org/10.1016/j.chemgeo.2019.01.019>
- Tian, S.H., Hou, Z.Q., Chen, X.Y., et al., 2020a. Magnesium Isotopic Behaviors between Metamorphic Rocks and Their Associated Leucogranites, and Implications for Himalayan Orogenesis. *Gondwana Research*, 87: 23–40. <https://doi.org/10.1016/j.gr.2020.06.006>
- Tipper, E.T., Calmels, D., Gaillardet, J., et al., 2012. Positive Correlation between Li and Mg Isotope Ratios in the River Waters of the Mackenzie Basin Challenges the Interpretation of Apparent Isotopic Fractionation during Weathering. *Earth and Planetary Science Letters*, 333/334:35–45. <https://doi.org/10.1016/j.epsl.2012.04.023>
- Tipper, E.T., Galy, A., Bickle, M.J., 2008. Calcium and Magnesium Isotope Systematics in Rivers Draining the Himalaya-Tibetan-Plateau Region: Lithological or Fractionation Control? *Geochimica et Cosmochimica Acta*, 72 (4):1057–1075
- Tipper, E.T., Galy, A., Gaillardet, J., et al., 2006. The Magnesium Isotope Budget of the Modern Ocean: Constraints from Riverine Magnesium Isotope Ratios. *Earth and Planetary Science Letters*, 250(1–2): 241–253. <https://doi.org/10.1016/j.epsl.2006.07.037>
- Twyman, J.D., Gittins, J., 1987. Alkalic Carbonatite Magmas: Parental or Derivative? *Geological Society, London, Special Publications*, 30(1): 85–94. <https://doi.org/10.1144/gsl.sp.1987.030.01.06>
- Urey, H.C., 1947. The Thermodynamic Properties of Isotopic Substances. *Journal of the Chemical Society (Resumed)*, 562–581. <https://doi.org/10.1039/jr9470000562>
- U.S. Geological Survey, 2018. Mineral Commodity Summaries 2018. National Minerals Information Center, Reston. <https://doi.org/10.3133/70194932>
- Vega, C.G.D., Chernozhkin, S.M., Grigoryan, R., et al., 2020. Characterization of the New Isotopic Reference Materials IRMM-524A and ERM-AE143 for Fe and Mg Isotopic Analysis of Geological and Biological Samples. *Journal of Analytical Atomic Spectrometry*, 35(11): 2517–2529. <https://doi.org/10.1039/d0ja00225a>
- Wang, D.H., 2019. Study on Critical Mineral Resources: Significance of Research, Determination of Types, Attributes

- of Resources, Progress of Prospecting, Problems of Utilization, and Direction of Exploitation. *Acta Geologica Sinica*, 93(6):1189–1209. <https://doi.org/10.19762/j.cnki.dizhixuebao.2019186>(in Chinese with English abstract).
- Wang, S. J., Teng, F. Z., Li, S. G., et al., 2014a. Magnesium Isotopic Systematics of Mafic Rocks during Continental Subduction. *Geochimica et Cosmochimica Acta*, 143:34–48. <https://doi.org/10.1016/j.gca.2014.03.029>
- Wang, S. J., Teng, F. Z., Li, S. G., 2014b. Tracing Carbonate-Silicate Interaction during Subduction Using Magnesium and Oxygen Isotopes. *Nature Communications*, 5: 5328. <https://doi.org/10.1038/ncomms6328>
- Wang, S. J., Teng, F. Z., Li, S. G., et al., 2017a. Tracing Subduction Zone Fluid-Rock Interactions Using Trace Element and Mg-Sr-Nd Isotopes. *Lithos*, 290–291: 94–103. <https://doi.org/10.1016/j.lithos.2017.08.004>
- Wang, X. J., Chen, L. H., Hofmann, A. W., et al., 2017b. Mantle Transition Zone-Derived EM1 Component beneath NE China: Geochemical Evidence from Cenozoic Potassic Basalts. *Earth and Planetary Science Letters*, 465: 16–28. <https://doi.org/10.1016/j.epsl.2017.02.028>
- Wang, W. Z., Qin, T., Zhou, C., et al., 2017c. Concentration Effect on Equilibrium Fractionation of Mg-Ca Isotopes in Carbonate Minerals: Insights from First-Principles Calculations. *Geochimica et Cosmochimica Acta*, 208: 185–197. <https://doi.org/10.1016/j.gca.2017.03.023>
- Wang, S. J., Teng, F. Z., Rudnick, R. L., et al., 2015a. The Behavior of Magnesium Isotopes in Low-Grade Metamorphosed Mudrocks. *Geochimica et Cosmochimica Acta*, 165: 435–448. <https://doi.org/10.1016/j.gca.2015.06.019>
- Wang, S. J., Teng, F. Z., Bea, F., 2015b. Magnesium Isotopic Systematics of Metapelite in the Deep Crust and Implications for Granite Petrogenesis. *Geochemical Perspectives Letters*, 1: 75–83. <https://doi.org/10.7185/geochemlet.1508>
- Wang, S. J., Teng, F. Z., Scott, J. M., 2016a. Tracing the Origin of Continental HIMU-Like Intraplate Volcanism Using Magnesium Isotope Systematics. *Geochimica et Cosmochimica Acta*, 185: 78–87. <https://doi.org/10.1016/j.gca.2016.01.007>
- Wang, Z. Z., Liu, S. G., Ke, S., et al., 2016b. Magnesium Isotopic Heterogeneity across the Cratonic Lithosphere in Eastern China and Its Origins. *Earth and Planetary Science Letters*, 451: 77–88. <https://doi.org/10.1016/j.epsl.2016.07.021>
- Wang, X. J., Chen, L. H., Hanyu, T., et al., 2021. Magnesium Isotopic Fractionation during Basalt Differentiation as Recorded by Evolved Magmas. *Earth and Planetary Science Letters*, 565: 116954. <https://doi.org/10.1016/j.epsl.2021.116954>
- Wang, X. J., Chen, L. H., Hofmann, A. W., et al., 2018. Recycled Ancient Ghost Carbonate in the Pitcairn Mantle Plume. *Proceedings of the National Academy of Sciences of the United States of America*, 115(35): 8682–8687. <https://doi.org/10.1073/pnas.1719570115>
- Wang, Z. Z., Liu, S. G., Liu, Z. C., et al., 2020. Extreme Mg and Zn Isotope Fractionation Recorded in the Himalayan Leucogranites. *Geochimica et Cosmochimica Acta*, 278: 305–321. <https://doi.org/10.1016/j.gca.2019.09.026>
- Watkins, J. M., DePaolo, D. J., Watson, E. B., 2017. Kinetic Fractionation of Non-Traditional Stable Isotopes by Diffusion and Crystal Growth Reactions. *Reviews in Mineralogy and Geochemistry*, 82(1):85–125. <https://doi.org/10.2138/rmg.2017.82.4>
- Wendlandt, R. F., Harrison, W. J., 1979. Rare Earth Partitioning between Immiscible Carbonate and Silicate Liquids and CO<sub>2</sub> Vapor: Results and Implications for the Formation of Light Rare Earth-Enriched Rocks. *Contributions to Mineralogy and Petrology*, 69(4): 409–419. <https://doi.org/10.1007/BF00372266>
- Wimpenny, J., Colla, C. A., Yin, Q. Z., et al., 2014a. Investigating the Behaviour of Mg Isotopes during the Formation of Clay Minerals. *Geochimica et Cosmochimica Acta*, 128: 178–194. <https://doi.org/10.1016/j.gca.2013.12.012>
- Wimpenny, J., Yin, Q. Z., Tollstrup, D., et al., 2014b. Using Mg Isotope Ratios to Trace Cenozoic Weathering Changes: A Case Study from the Chinese Loess Plateau. *Chemical Geology*, 376: 31–43. <https://doi.org/10.1016/j.chemgeo.2014.03.008>
- Woolley, A. R., Kjarsgaard, B. A., 2008. Paragenetic Types of Carbonatite as Indicated by the Diversity and Relative Abundances of Associated Silicate Rocks: Evidence from a Global Database. *The Canadian Mineralogist*, 46(4):741–752. <https://doi.org/10.3749/canmin.46.4.741>
- Wu, H. J., He, Y. S., Teng, F. Z., et al., 2018. Diffusion-Driven Magnesium and Iron Isotope Fractionation at a Gabbro-Granite Boundary. *Geochimica et Cosmochimica Acta*, 222: 671–684. <https://doi.org/10.1016/j.gca.2017.11.010>
- Xiang, M., Gong, Y. L., Liu, T., et al., 2021. New Advances in Calcium Isotope Geochemistry and Its Application to Carbonatite and Associated Silicate Rocks. *Acta Geologica Sinica*(in press)(in Chinese with English abstract).
- Xiao, Y., Teng, F. Z., Su, B. X., et al., 2016. Iron and Magnesium Isotopic Constraints on the Origin of Chemical Heterogeneity in Podiform Chromitite from the Luobusa

- Ophiolite, Tibet. *Geochemistry, Geophysics, Geosystems*, 17(3):940–953. <https://doi.org/10.1002/2015gc006223>
- Xiao, Y., Teng, F.Z., Zhang, H.F., et al., 2013. Large Magnesium Isotope Fractionation in Peridotite Xenoliths from Eastern North China Craton: Product of Melt–Rock Interaction. *Geochimica et Cosmochimica Acta*, 115: 241–261. <https://doi.org/10.1016/j.gca.2013.04.011>
- Xiao, Y.L., Sun, H., Gu, H.O., et al., 2015. Fluid/Melt in Continental Deep Subduction Zones: Compositions and Related Geochemical Fractionations. *Science China: Earth Sciences*, 45: 1063–1087 (in Chinese).
- Xie, L.W., Yin, Q.Z., Yang, J.H., et al., 2011. High Precision Analysis of Mg Isotopic Composition in Olivine by Laser Ablation MC-ICP-MS. *Journal of Analytical Atomic Spectrometry*, 26(9): 1773–1780. <https://doi.org/10.1039/c1ja10034c>
- Xie, Q.H., Zhang, Z.C., Campos, E., et al., 2018. Magnesium Isotopic Composition of Continental Arc Andesites and the Implications: A Case Study from the El Laco Volcanic Complex, Chile. *Lithos*, 318–319: 91–103. <https://doi.org/10.1016/j.lithos.2018.08.010>
- Xie, Y.L., Hou, Z.Q., Goldfarb, R.J., et al., 2016. Rare Earth Element Deposits in China. Rare Earth and Critical Elements in Ore Deposits. *Reviews in Economic Geology*, 18: 115–136. <https://doi.org/10.5382/rev.18.06>
- Xie, Y.L., Qu, Y.W., Yang, Z.F., et al., 2019. Giant Bayan Obo Fe–Nb–REE Deposit: Progresses, Controversies and New Understandings. *Mineral Deposits*, 38(5): 983–1003 (in Chinese with English abstract).
- Xie, Y.L., Verplanck, P.L., Hou, Z.Q., et al., 2020. Rare Earth Element Deposits in China: A Review and New Understandings. In: Chang, Z., Goldfarb, R.J., eds., *Mineral Deposits of China*, Volume SEG Special Publications. Society of Economic Geologists, Inc., Kansas, 22: 509–552.
- Xie, Y.L., Xia, J.M., Cui, K., et al., 2020. Rare Earth Elements Deposits in China: Spatio-Temporal Distribution and Ore-Forming Processes. *Chinese Science Bulletin*, 65(33): 3794–3808 (in Chinese).
- Xu, C., Chakhmouradian, A.R., Taylor, R.N., et al., 2014. Origin of Carbonatites in the South Qinling Orogen: Implications for Crustal Recycling and Timing of Collision between the South and North China Blocks. *Geochimica et Cosmochimica Acta*, 143: 189–206. <https://doi.org/10.1016/j.gca.2014.03.041>
- Xu, C., Taylor, R.N., Kynicky, J., et al., 2011. The Origin of Enriched Mantle beneath North China Block: Evidence from Young Carbonatites. *Lithos*, 127(1–2): 1–9. <https://doi.org/10.1016/j.lithos.2011.07.021>
- Yang, K.F., Fan, H.R., Pirajno, F., et al., 2019. The Bayan Obo (China) Giant REE Accumulation Conundrum Elucidated by Intense Magmatic Differentiation of Carbonate. *Geology*, 47(12): 1198–1202. <https://doi.org/10.1130/g46674.1>
- Yang, W., Teng, F.Z., Li, W.Y., et al., 2016. Magnesium Isotopic Composition of the Deep Continental Crust. *American Mineralogist*, 101(2): 243–252. <https://doi.org/10.2138/am-2016-5275>
- Yang, W., Teng, F.Z., Zhang, H.F., 2009. Chondritic Magnesium Isotopic Composition of the Terrestrial Mantle: A Case Study of Peridotite Xenoliths from the North China Craton. *Earth and Planetary Science Letters*, 288(3–4): 475–482. <https://doi.org/10.1016/j.epsl.2009.10.009>
- Yang, W., Teng, F.Z., Zhang, H.F., et al., 2012. Magnesium Isotopic Systematics of Continental Basalts from the North China Craton: Implications for Tracing Subducted Carbonate in the Mantle. *Chemical Geology*, 328: 185–194. <https://doi.org/10.1016/j.chemgeo.2012.05.018>
- Zhai, M.G., Wu, F.Y., Hu, R.Z., et al., 2019. Critical Metal Mineral Resources: Current Research Status and Scientific Issues. *Bulletin of National Natural Science Foundation of China*, 33(2): 106–111 (in Chinese with English abstract).
- Zhang, G.L., Chen, L.H., Jackson, M.G., et al., 2017. Evolution of Carbonated Melt to Alkali Basalt in the South China Sea. *Nature Geoscience*, 10(3): 229–235. <https://doi.org/10.1038/ngeo2877>
- Zhang, H.F., Tang, Y.J., Zhao, X.M., et al., 2007. Significance and Prospective of Non-Traditional Isotopic Systems in Mantle Geochemistry. *Earth Science Frontiers*, 14(2): 37–57 (in Chinese with English abstract).
- Zhao, T., Liu, W.J., Xu, Z.F., et al., 2019. The Influence of Carbonate Precipitation on Riverine Magnesium Isotope Signals: New Constraints from Jinsha River Basin, Southeast Tibetan Plateau. *Geochimica et Cosmochimica Acta*, 248: 172–184. <https://doi.org/10.1016/j.gca.2019.01.005>
- Zhong, Y., Chen, L.H., Wang, X.J., et al., 2017. Magnesium Isotopic Variation of Oceanic Island Basalts Generated by Partial Melting and Crustal Recycling. *Earth and Planetary Science Letters*, 463: 127–135. <https://doi.org/10.1016/j.epsl.2017.01.040>
- Zhong, Y., Zhang, G.L., Jin, Q.Z., et al., 2021. Sub-Basin Scale Inhomogeneity of Mantle in the South China Sea Revealed by Magnesium Isotopes. *Science Bulletin*, 66(7): 740–748. <https://doi.org/10.1016/j.scib.2020.12.016>
- Zhu, X.K., Wang, Y., Yan, B., et al., 2013. Developments of Non-Traditional Stable Isotope Geochemistry. *Bulletin*

of Mineralogy, Petrology and Geochemistry, 32(6):651—688(in Chinese with English abstract).

### 附中文参考文献

- 陈伊翔, 2019. 大陆俯冲隧道板片—地幔楔界面反向流体交代作用: 西阿尔卑斯造山带超高压变质白片岩的地球化学证据. 地球科学, 44(12):4057—4063.
- 戴梦宁, 包志安, 陈开运, 等, 2016. 飞秒激光剥蚀—多接收等离子体质谱原位分析玄武岩玻璃样品 Mg 同位素组成. 分析化学, 44(2):173—178.
- 董爱国, 韩贵琳, 2017. 镁同位素体系在河流中的研究进展. 地球科学进展, 32(8):800—809.
- 董爱国, 朱祥坤, 2016. 表生环境中镁同位素的地球化学循环. 地球科学进展, 31(1):43—58.
- 范百龄, 陶发祥, 赵志琦, 2013. 地表及海洋环境的镁同位素地球化学研究进展. 矿物岩石地球化学通报, 32(1):114—120.
- 范宏瑞, 牛贺才, 李晓春, 等, 2020. 中国内生稀土矿床类型、成矿规律与资源展望. 科学通报, 65(33):3778—3793.
- 何学贤, 朱祥坤, 李世珍, 等, 2008. 多接收器等离子体质谱(MC-ICP-MS)测定 Mg 同位素方法研究. 岩石矿物学杂志, 27(5):441—448.
- 侯增谦, 陈骏, 翟明国, 2020. 战略性关键矿产研究现状与科学前沿. 科学通报, 65(33):3651—3652.
- 黄建, 黄方, 肖益林, 2019. 蚀变洋壳和俯冲带变质流体的 Fe-Mg 同位素组成. 地球科学, 44(12):4050—4056. <https://doi.org/10.3799/dqkx.2019.234>
- 蒋少涌, 温汉捷, 许成, 等, 2019. 关键金属元素的多圈层循环与富集机理: 主要科学问题及未来研究方向. 中国科学基金, 33(2):112—118.
- 柯珊, 刘盛遨, 李王晔, 等, 2011. 镁同位素地球化学研究新进展及其应用. 岩石学报, 27(2):383—397.
- 李瑞瑛, 柯珊, 何永胜, 等, 2016. 高 Cr 地质样品的 Mg 同位素分析方法. 矿物岩石地球化学通报, 35(3):441—447.
- 李世珍, 朱祥坤, 何学贤, 等, 2008. 用于多接收器等离子质谱 Mg 同位素测定的分离方法研究. 岩石矿物学杂志, 27(5):449—456.
- 李曙光, 2015. 深部碳循环的 Mg 同位素示踪. 地学前缘, 22(5):143—159.
- 李伟强, 赵书高, 王小敏, 等, 2020. 斑岩铜矿热液流体的 K-

- Mg 同位素示踪. 中国科学:地球科学, 50(2):245—257.
- 刘琰, 陈超, 舒小超, 等, 2017. 青藏高原东部碳酸岩—正长岩杂岩体 REE 矿床成矿模式: 以大陆槽 REE 矿床为例. 岩石学报, 33(7):1978—2000.
- 毛景文, 袁顺达, 谢桂青, 等, 2019. 21 世纪以来中国关键金属矿产找矿勘查与研究新进展. 矿床地质, 38(5):935—969.
- 沈骥, 李王晔, 李曙光, 等, 2019. 俯冲隧道内不同深度的壳幔相互作用: 地幔楔超镁铁质岩的镁同位素记录. 地球科学, 44(12):4102—4111.
- 宋文磊, 许成, 王林均, 等, 2013. 与碳酸岩碱性杂岩体相关的内生稀土矿床成矿作用研究进展. 北京大学学报(自然科学版), 49(4):725—740.
- 苏本勋, 肖燕, 陈晨, 等, 2018. Fe-Mg 同位素在蛇绿岩中铬铁矿床成因研究中的应用潜力. 地球科学, 43(4):1011—1024. <https://doi.org/10.3799/dqkx.2018.705>
- 孙剑, 朱祥坤, 陈岳龙, 等, 2012. 白云鄂博地区相关地质单元的铁同位素特征及其对白云鄂博矿床成因的制约. 地质学报, 86(5):819—828.
- 王登红, 2019. 关键矿产的研究意义、矿种厘定、资源属性、找矿进展、存在问题及主攻方向. 地质学报, 93(6):1189—1209.
- 向蜜, 龚迎莉, 刘涛, 等, 2021. 钙同位素地球化学研究新进展及其在碳酸岩—共生硅酸盐研究中的应用. 地质学报(待刊).
- 肖益林, 孙贺, 顾海欧, 等, 2015. 大陆深俯冲过程中的熔/流体成分与地球化学分异. 中国科学:地球科学, 45(8):1063—1087.
- 谢玉玲, 曲云伟, 杨占峰, 等, 2019. 白云鄂博铁、钕、稀土矿床: 研究进展、存在问题和新认识. 矿床地质, 38(5):983—1003.
- 谢玉玲, 夏加明, 崔凯, 等, 2020. 中国碳酸岩型稀土矿床: 时空分布与成矿过程. 科学通报, 65(33):3794—3808.
- 翟明国, 吴福元, 胡瑞忠, 等, 2019. 战略性关键金属矿产资源: 现状与问题. 中国科学基金, 33(2):106—111.
- 张宏福, 汤艳杰, 赵新苗, 等, 2007. 非传统同位素体系在地幔地球化学研究中的重要性及其前景. 地学前缘, 14(2):37—57.
- 朱祥坤, 王跃, 闫斌, 等, 2013. 非传统稳定同位素地球化学的创建与发展. 矿物岩石地球化学通报, 32(6):651—688.